Available online at www.sciencedirect.com

ScienceDirect

Nuclear Physics B 996 (2023) 116353

NUCLEAR PHYSICS B

www.elsevier.com/locate/nuclphysb

Quantum Field Theory and Statistical Systems

Ferromagnetic phase transitions in $SU(N)$

Alexios P. Polychronakos [a,b,*], Konstantinos Sfetsos [c,d]

[a] *Physics Department, the City College of the New York, 160 Convent Avenue, New York, NY 10031, USA*
[b] *The Graduate School and University Center, City University of New York, 365 Fifth Avenue, New York, NY 10016, USA*
[c] *Department of Nuclear and Particle Physics, Faculty of Physics, National and Kapodistrian University of Athens, Athens 15784, Greece*
[d] *Theoretical Physics Department, CERN, 1211 Geneva 23, Switzerland*

Received 12 June 2023; received in revised form 13 August 2023; accepted 8 September 2023
Available online 25 September 2023
Editor: Hubert Saleur

Abstract

We study the thermodynamics of a non-abelian ferromagnet consisting of "atoms" each carrying a fundamental representation of $SU(N)$, coupled with long-range two-body quadratic interactions. We uncover a rich structure of phase transitions from non-magnetized, global $SU(N)$-invariant states to magnetized ones breaking global invariance to $SU(N-1) \times U(1)$. Phases can coexist, one being stable and the other metastable, and the transition between states involves latent heat exchange, unlike in usual $SU(2)$ ferromagnets. Coupling the system to an external non-abelian magnetic field further enriches the phase structure, leading to additional phases. The system manifests hysteresis phenomena both in the magnetic field, as in usual ferromagnets, and in the temperature, in analogy to supercooled water. Potential applications are in fundamental situations or as a phenomenological model.

Contents

* Corresponding author.
E-mail addresses: apolychronakos@ccny.cuny.edu, apolychronakos@gc.cuny.edu (A.P. Polychronakos), ksfetsos@phys.uoa.gr (K. Sfetsos).

https://doi.org/10.1016/j.nuclphysb.2023.116353

1. Introduction

Magnetic materials are of considerable physical and technological interest, and their properties have long been the subject of theoretical research. Ferromagnets, the first type of magnetism ever observed, hold a special place among them, as they manifest nontrivial properties and symmetry breaking.

All known ferromagnets consist of interacting localized magnetic dipoles and break rotational invariance below the Curie temperature. Each (quantum) dipole provides a representation of the group of rotations, that is, of $SU(2)$. Although this is a nonabelian group, it is of a particularly simple type: it has a unique Cartan generator, and $SU(2)$ dipoles can interact with external abelian magnetic fields that couple to their Cartan generator. Nevertheless, the exact quantitative properties of physical ferromagnets remain an active topic of research [1].

Independently, nonabelian unitary groups $SU(N)$ of higher rank play a crucial role in particle physics and, indirectly through matrix models, in string theory and gravity. Ungauged and gauged $SU(3)$ groups are the most common, representing "flavor" and "color" degrees of freedom, respectively. A collection of nucleons, or the constituents of the quark-gluon plasma, are physical systems of components carrying representations of $SU(3)$. This raises the obvious question of the properties that large collections of such $SU(3)$ or, more generally, $SU(N)$ entities would have if they interacted with each other as well as with external nonabelian magnetic fields.

In this work we investigate the properties of such systems in the ferromagnetic regime, that is, in the regime where the mutual interaction of its components would tend to "align" their $SU(N)$ charges, in a way that we will make precise. The results on the decomposition of the

direct product of an arbitrary number of representations of $SU(N)$ into irreducible components that we derived in a recent publication [2] will be a crucial tool in our calculations. We will also study the effects of an external nonabelian magnetic field coupled to the system. As we shall demonstrate, the properties of nonabelian ($N > 2$) ferromagnets are qualitatively different from these of ordinary ($N = 2$) ferromagnets. They display a rich phase structure involving various critical temperatures, hysteresis both in the temperature and in the magnetic field, coexistence of phases, and latent heat transfer during phase transitions.

In the sequel we will present the basic $SU(N)$ model, consisting of distinguishable quantum components in the fundamental representation, and will review the relevant group theory results of [2]. We will proceed to study the thermodynamic phases of the model in the absence, and subsequently in the presence, of external magnetic fields, and will derive its symmetry breaking patterns, critical temperatures, and magnetization. Stability issues will be crucial and will determine the pattern of $SU(N)$ breaking in the various phases. We will further study the nontrivial situation of a magnetic field inducing an enhanced breaking of $SU(N)$, and will conclude with some speculations about the phenomenological relevance of the model.

2. A system of interacting $SU(N)$ "atoms"

Magnetic systems with $SU(N)$ symmetry have been considered in the context of ultracold atoms [3–7] or of interacting atoms on lattice cites [8–14] and in the presence of $SU(N)$ magnetic fields [15–17].

In this section we lay out the basic structure of any model of interacting $SU(N)$ atoms, specify its ferromagnetic regime, and review the group theory results necessary for its analytic treatment.

2.1. The model

To motivate the basic model, consider a set of n atoms (or molecules) on a lattice, interacting with two-body interactions. Each atom is in one of N degenerate or quasi-degenerate states $|s\rangle$, $s = 1, 2, \ldots, N$. The generic two-body interaction between atoms 1 and 2 with states $|s_1\rangle$ and $|s_2\rangle$ would be

$$H_{12} = \sum_{s_1,s_1',s_2,s_2'=1}^{N} h_{s_1 s_2; s_1' s_2'} \, |s_1\rangle \, \langle s_1'| \otimes |s_2\rangle \, \langle s_2'| \ , \qquad h_{s_1 s_2; s_1' s_2'} = h^*_{s_1' s_2'; s_1 s_2} \ . \tag{2.1}$$

Define j_a, $a = 0, 1, \ldots, N^2 - 1$, the generators of $U(N)$ in the fundamental N-dimensional representation, with j_0 the identity operator (the $U(1)$ part). Using the fact that the j_a form a complete basis for the operators acting on an N-dimensional space, the above interaction can also be written as

$$H_{12} = \sum_{a,b=0}^{N^2-1} h_{ab} \, j_{1,a} \, j_{2,b} \ , \qquad h_{ab} = h^*_{ab} \ , \tag{2.2}$$

where

$$j_{1,a} = j_a \otimes 1 \ , \qquad j_{2,a} = 1 \otimes j_a \ , \tag{2.3}$$

are the fundamental $U(N)$ operators acting on the states of atoms 1 and 2.

We now make the physical assumption that the above interaction is invariant under a change of basis in the states $|s\rangle$, that is, under a common unitary transformation of the states $|s_1\rangle$ of atom 1 and $|s_2\rangle$ of atom 2. This implies two equivalent facts: first, the interaction will necessarily be, up to trivial additive and multiplicative constants (proportional to the identity), the operator exchanging the states of the atoms,

$$H_{12} = C'_{12} + C_{12} \sum_{s,s'=1}^{N} |s\rangle \langle s'| \otimes |s'\rangle \langle s| \ , \tag{2.4}$$

with C'_{12}, C_{12} being real constants. Second, the interaction will necessarily be of the form

$$H_{12} = c'_{12} + c_{12} \sum_{a=1}^{N^2-1} j_{1,a}\, j_{2,a} \ . \tag{2.5}$$

Omitting the trivial constant c'_{12} (due to the $U(1)$ part), we obtain a unique two-body interaction depending on a single coupling constant c_{12}. Note that the group $U(N)$ emerges from the requirement of invariance under general changes of basis of the N states, and leads to interactions linear in the operators in each atom. Using, instead, an N-dimensional representation of a smaller group would require the inclusion of higher polynomial terms in $j_{1,a}$ and $j_{2,a}$.

The interaction Hamiltonian of the full system will be of the form

$$H = \sum_{r,s=1}^{n} c_{rs} \sum_{a=1}^{N^2-1} j_{r,a}\, j_{s,a} \ , \tag{2.6}$$

where $c_{rs} = c_{sr}$ is the strength of the interaction between atoms r and s (and $c_{rr} = 0$). This Hamiltonian involves an isotropic quadratic coupling between the fundamental generators of the n commuting $SU(N)$ groups of the atoms.

Reasonable physical assumptions restrict the form of the couplings c_{rs}. We assume that the interaction is homogeneous, that is, c_{rs} is translationally invariant under the shift of both r and s by the same lattice translation (away from the boundary of the lattice). In terms of the lattice positions of the atoms $\vec{r}$,

$$c_{\vec{r},\vec{s}} = c_{\vec{r}-\vec{s}} \ , \qquad c_0 = 0 \ . \tag{2.7}$$

Therefore, each atom couples to a fixed weighted average of the $SU(N)$ generators of its neighboring atoms. We will also assume that interactions are reasonably long-range, that is, each atom couples to several of its neighboring atoms. This technical assumption justifies the mean field condition that, in the thermodynamic limit, the weighted average of the neighboring atoms is well approximated by their average over the full lattice. That is

$$\sum_{\vec{s}} c_{\vec{s}}\, j_{\vec{r}+\vec{s},a} \simeq \Big(\sum_{\vec{s}} c_{\vec{s}}\Big) \frac{1}{n} \sum_{s=1}^{n} j_{s,a} = -\frac{c}{n} J_a \ , \tag{2.8}$$

where we defined the total $SU(N)$ generator

$$J_a = \sum_{s=1}^{n} j_{s,a} \tag{2.9}$$

and the effective mean coupling[1]

$$c = -\sum_{\vec{s}} c_{\vec{s}} \ . \tag{2.10}$$

The minus sign is introduced such that ferromagnetic interactions, driving atom states to align, correspond to positive c. Altogether, the full effective interaction assumes the form

$$H = -\frac{c}{n} \sum_{a=1}^{N^2-1} \left(J_a^2 - \sum_{s=1}^{n} j_{s,a}^2 \right) , \tag{2.11}$$

where the second term in the parenthesis eliminates the terms $r = s$. The first part of H is proportional to the quadratic Casimir of the total $SU(N)$ group $C^{(2)} = \sum_a J_a^2$. The second part is proportional to the sum of the quadratic Casimirs of each individual atom. Since all $j_{s,a}$ are in the fundamental representation, their quadratic Casimir is a (common) constant, independent of their state. So the second term contributes a trivial constant and can be discarded.

In addition to the atoms' mutual interaction, we can couple the states of the atoms to a global external field, contributing an additional term

$$H_B = \sum_{r=1}^{n} \sum_{s,s'=1}^{N} B_{ss'} \, |s\rangle_r \, \langle s'|_r \ . \tag{2.12}$$

Parametrizing this one-atom operator in terms of the complete set of operators $j_{r,a}$ and omitting the trivial constant terms corresponding to $j_{r,0}$, it becomes

$$H_B = \sum_{r=1}^{n} \sum_{a=1}^{N^2-1} B_a \, j_{r,a} = \sum_{a=1}^{N^2-1} B_a J_a \ . \tag{2.13}$$

We see that B_a acts as a global nonabelian magnetic field on the $SU(N)$ "spins" $j_{r,a}$. Finally, making use of the fact that the interaction Hamiltonian is invariant under global $SU(N)$ transformations, we may choose a basis of states in which the sum $\sum_a B_a J_a$ is rotated to the Cartan subspace spanned by the commuting generators H_i, $i = 1, 2, \ldots, N-1$. The full Hamiltonian of the model then emerges as

$$H = -\frac{c}{n} C^{(2)} - \sum_{i=1}^{N-1} B_i H_i \ . \tag{2.14}$$

We will assume that c is positive, so that the model is of the ferromagnetic type.

For $N = 2$ the above model reduces to the ferromagnetic interaction of spin-half components. For higher N, the model has the same number of states per atom as a spin-S $SU(2)$ model with $2S + 1 = N$. The dynamics of the two models, however, are distinct: the $SU(2)$ model is invariant only under global $SU(2)$ transformations, which cannot mix the N states of the atoms in an arbitrary way, unlike the $SU(N)$ case. The enhanced symmetry of the $SU(N)$ model leads, as we shall see, to a richer structure and to qualitatively different thermodynamic properties.

[1] The validity of the mean field approximation is strongest in three dimensions, since every atom has a higher number of near neighbors and the statistical fluctuations of their averaged coupling are weaker, but is expected to hold also in lower dimensions.

Finding the eigenstates of the above model and determining its thermodynamics involves decomposing the full Hilbert space of states into irreducible representations (irreps) of the total $SU(N)$, evaluating the quadratic Casimir $C^{(2)}$ and the magnetic sum $\sum_i B_i H_i$ in each irrep, and calculating the partition function as a sum over these irreps. This requires determining the decomposition of the direct product of a large, arbitrary number n of $SU(N)$ fundamentals into irreps and the multiplicity of each irrep in the decomposition, as well as calculating the Casimir and the magnetic sum for large irreps of $SU(N)$. This task was performed in a recent publication [2], and the relevant results will be reviewed in the next subsection.

2.2. Decomposition of n fundamentals of $SU(N)$ into irreps

We summarize the group theory results pertaining to the decomposition of the direct product of n fundamentals of $SU(N)$ into irreps, as presented in [2] (results on the simpler case of $SU(2)$ were previously derived in [18,19] and were applied in [18] to regular ferromagnetism).

The setting and results become most tractable and intuitive in the momentum representation, in which irreps of $SU(N)$ are labeled by a set of distinct integers k_i, $i = 1, 2, \ldots, N$ ordered as

$$k_1 > k_2 > \cdots > k_N \ . \tag{2.15}$$

Each irrep corresponds to a given set $\{k_i\}$, for which we will use the symbol $\mathbf{k}$. The corresponding Young Tableaux (YT) of the irrep may be described by its lengths ℓ_i, i.e., number of boxes per row, for $i = 1, 2, \ldots, N-1$. The correspondence with k_i is

$$\ell_i = k_i - k_N + i - N \ , \qquad \ell_1 \geqslant \ell_2 \geqslant \cdots \geqslant \ell_{N-1} \geqslant 0 \ . \tag{2.16}$$

Note that the k_i representation is redundant, since a shift of all k_i by a common constant $k_i \to k_i + c$ leaves ℓ_i invariant and leads to the same irrep of $SU(N)$ (the shift changes the $U(1)$ charge of the irrep, which equals the sum of the k_i). This freedom can be used to simplify relevant formulae. In our situation, where irreps will arise from the direct product of n fundamentals, it will be convenient to choose the convention

$$\sum_{i=1}^{N} k_i = n + \frac{N(N-1)}{2} \ . \tag{2.17}$$

For the singlet representation ($n = 0$) all ℓ_i are zero, which in the above convention corresponds to $k_i = N - i$, $i = 1, 2, \ldots, N$. The fundamental ($n = 1$) has a single box, and corresponds to $k_1 = N$ and the rest of the k_i as above.

In $SU(N)$ there are $N-1$ Casimir operators which, for the irrep $\mathbf{k}$, can be expressed in terms of the k_i's. For our purposes we need the quadratic Casimir, which is given in terms of the k_i by

$$C^{(2)}(\mathbf{k}) = \frac{1}{2}\sum_{i=1}^{N} k_i^2 - \frac{1}{2N}\,[n + N(N-1)/2]^2 - \frac{N(N^2-1)}{24} \ . \tag{2.18}$$

Note that, using (2.16), (2.17), $C^{(2)}$ takes the more familiar form

$$C^{(2)}(\ell) = \frac{1}{2}\sum_{i=1}^{N-1} \ell_i(\ell_i + N + 1 - 2i) - \frac{1}{2N}\left(\sum_{i=1}^{N-1} \ell_i\right)^2 \ . \tag{2.19}$$

For the singlet $C^{(2)} = 0$, while for the fundamental $C^{(2)} = (N - N^{-1})/2$.

For our purposes we also need the trace of the exponential of the magnetic term in a giver irrep $\mathbf{k}$,

$$\mathrm{Tr}_{\mathbf{k}} \exp\Big(\beta \sum_{j=1}^{N} B_j H_j\Big) \,, \tag{2.20}$$

which will appear in the calculation of the partition function of our model. This was calculated in [2]. To express it, define the Slater determinant

$$\psi_{\mathbf{k}}(\mathbf{z}) = (z_1 \cdots z_N)^{-\frac{1}{N}\sum_i k_i} \begin{vmatrix} z_1^{k_1} & z_1^{k_2} & \cdots & z_1^{k_{N-1}} & z_1^{k_N} \\ z_2^{k_1} & z_2^{k_2} & \cdots & z_2^{k_{N-1}} & z_2^{k_N} \\ \vdots & \vdots & \ddots & \vdots & \vdots \\ z_N^{k_1} & z_N^{k_2} & \cdots & z_N^{k_{N-1}} & z_N^{k_N} \end{vmatrix} \,, \qquad \mathbf{z} = \{z_i \in \mathbb{C}\} \,, \tag{2.21}$$

which is antisymmetric under the interchange of any two z_i's and of any two k_i's. Also define the Vandermonde determinant

$$\Delta(\mathbf{z}) = (z_1 \cdots z_N)^{-\frac{N-1}{2}} \begin{vmatrix} z_1^{N-1} & z_1^{N-2} & \cdots & z_1 & 1 \\ z_2^{N-1} & z_2^{N-2} & \cdots & z_2 & 1 \\ \vdots & \vdots & \ddots & \vdots & \vdots \\ z_N^{N-1} & z_N^{N-2} & \cdots & z_N & 1 \end{vmatrix} \,, \tag{2.22}$$

which is the Slater determinant (2.21) for the singlet irrep. Then

$$\mathrm{Tr}_{\mathbf{k}} \exp\Big(\beta \sum_{j=1}^{N} B_j H_j\Big) = \frac{\psi_{\mathbf{k}}(\mathbf{z})}{\Delta(\mathbf{z})} \,, \qquad z_j = e^{\beta B_j} \,. \tag{2.23}$$

The prefactors involving the product $z_1 \cdots z_N$ in (2.21) and (2.22) eliminate the $U(1)$ part of the irrep, which couples to the trace of the magnetic field $\sum_i B_i$. If B is traceless, then the $U(1)$ charge decouples and we can ignore these prefactors. As a check of (2.23), we can take the limit $z_i \to 1$ and verify that the ratio of determinants goes to

$$\mathrm{Tr}_{\mathbf{k}} \mathbf{1} = \dim(\mathbf{k}) = \prod_{j>i=1}^{N} \frac{k_i - k_j}{j-i} = \prod_{j>i=1}^{N} \frac{\ell_i - \ell_j + j - i}{j-i} \,, \tag{2.24}$$

which is the standard expression for the dimension of the irrep.

The last nontrivial element needed for our purposes is the multiplicity $d_{n,\mathbf{k}}$ of each irrep $\mathbf{k}$ arising in the decomposition of n fundamental representations. This was also calculated in [2], and the result is

$$\begin{aligned} d_{n,\mathbf{k}} &= \delta_{k_1+\cdots+k_N,n+N(N-1)/2} \prod_{j>i=1}^{N} (S_i - S_j) D_{n,\mathbf{k}} \,, \\ D_{n,\mathbf{k}} &= \frac{n!}{\prod_{r=1}^{N} k_r!} \,, \end{aligned} \tag{2.25}$$

where S_i is a shift operator acting on the right by replacing k_i by $k_i - 1$. Note that $D_{n,\mathbf{k}}$ and $d_{n,\mathbf{k}}$ are manifestly symmetric and antisymmetric, respectively, under exchange of the k_i. In [2] the

action of the operator $\prod_{j>i=1}^{N}(S_i - S_j)$ on $D_{n,\mathbf{k}}$ was performed and an explicit combinatorial formula for $d_{n,\mathbf{k}}$ was obtained, but it will not be needed for our purposes.

2.3. The thermodynamic limit of the model

We now have all the ingredients to study the statistical mechanics of our $SU(N)$ ferromagnet. The partition function is

$$Z = \sum_{\text{states}} e^{-\beta H} = \sum_{<\mathbf{k}>} d_{n;\mathbf{k}}\, e^{\frac{\beta c}{n} C^{(2)}(\mathbf{k})}\, \mathrm{Tr}_{\mathbf{k}} \exp\Big(\beta \sum_{j=1}^{N} B_j H_j\Big)\,, \tag{2.26}$$

where β is the inverse of the temperature T and $<\mathbf{k}>$ denotes distinct ordered integers $k_1 > k_2 > \cdots > k_N$ satisfying the constraint (2.17). Using the results (2.18), (2.23) and (2.25), and removing the trivial (k_i-independent) terms in the Casimir (2.18), the partition function becomes

$$\begin{aligned} Z =& \frac{1}{N!} \sum_{\mathbf{k}} \delta_{k_1+\cdots+k_N, n+\frac{N(N-1)}{2}} \Big(\prod_{j>i=1}^{N} (S_i - S_j) \frac{n!}{\prod_{r=1}^{N} k_r!} \Big) \frac{\psi_{\mathbf{k}}(\mathbf{z})}{\Delta(\mathbf{z})}\, e^{\frac{\beta c}{2n}\sum_s k_s^2} \\ =& \sum_{\mathbf{k}} \delta_{k_1+\cdots+k_N, n+\frac{N(N-1)}{2}} \frac{1}{\Delta(\mathbf{z})} \Big(\prod_{j>i=1}^{N} (S_i - S_j) \frac{n!}{\prod_{r=1}^{N} k_r!} \Big) e^{\frac{\beta c}{2n}\sum_s k_s^2 + \beta B_s k_s} \\ =& \sum_{\mathbf{k}} \delta_{k_1+\cdots+k_N, n} \frac{1}{\Delta(\mathbf{z})} \frac{n!}{\prod_{r=1}^{N} k_r!} \prod_{j>i=1}^{N} \big(S_i^{-1} - S_j^{-1}\big)\, e^{\frac{\beta c}{2n}\sum_s k_s^2 + \beta B_s k_s}\,. \end{aligned} \tag{2.27}$$

In the first line above we made the sum unrestricted, since the summand is symmetric under permutation of the k_i and vanishes for $k_i = k_j$, and introduced the constraint explicitly. The second line follows since $d_{n,\mathbf{k}}$ (the expression in the parenthesis) is antisymmetric in the k_i, and thus it picks the fully antisymmetric part of $z_1^{k_1}\cdots z_N^{k_N}$, reproducing $\psi_{\mathbf{k}}(\mathbf{z})$. The third line is obtained by shifting summation variables. In doing so, the factor $N(N-1)/2$ in the Kronecker δ is absorbed.

The above holds for arbitrary n. We now take the thermodynamic limit $n \gg 1$. The typical k_i is of order n, and thus the exponent in the expression is of order n, and any prefactor polynomial in n is irrelevant, as is the factor $\Delta(\mathbf{z})$. Similarly, the action of $\prod_{j>i}(S_i^{-1} - S_j^{-1})$ produces a subleading factor that can be ignored (one way to see this is to note that in the large n limit the shift operators act as derivatives ($S_i^{-1} - S_j^{-1} \simeq \partial_{k_i} - \partial_{k_j}$) and bring down subleading terms). Further, we apply to $k_r!$ the Stirling approximation. Altogether we obtain

$$Z = \sum_{\mathbf{k}} \delta_{k_1+\cdots+k_N, n} e^{-\beta\, \mathrm{F}(\mathbf{k}) + \mathcal{O}(n^0)}\,, \tag{2.28}$$

where the free energy of the system is, up to a trivial overall constant,

$$\mathrm{F}(\mathbf{k}) = -Tn\ln n + \sum_{i=1}^{N} \Big(T k_i \ln k_i - \frac{c}{2n} k_i^2 - B_i k_i \Big)\,. \tag{2.29}$$

In the large-n limit, quantities k_i and F are extensive variables of order n. We will now transition to intensive variables, that is, quantities per atom. To this end, we define rescaled variables x_i as

$$k_i = nx_i \ , \quad i = 1, 2, \ldots, N \ . \tag{2.30}$$

satisfying the constraint

$$\sum_{i=1}^{N} x_i = 1 \ . \tag{2.31}$$

In terms of the x_i, the non-extensive term $-Tn \ln n$ in the free energy cancels and F becomes properly extensive,

$$\mathrm{F}(\mathbf{x}) = n \sum_{i=1}^{N} \Big(T x_i \ln x_i - \frac{NT_0}{2} x_i^2 - B_i x_i \Big) = n F(\mathbf{x}) \ , \tag{2.32}$$

where we have defined

$$c = NT_0 \ , \tag{2.33}$$

introducing a temperature scale T_0. From now on we will work with the intensive quantities x_i (magnetization per atom) and F (free energy per atom) and will omit the qualifier "per atom".

In the large-n limit the sum in (2.28) can be obtained by a saddle-point approximation, as the exponent is of order n, by minimizing the free energy $F(\mathbf{x})$ while respecting the constraint $\sum_{i=1}^{N} x_i = 1$. This can be done with a Lagrange multiplier. Adding the term $\lambda(1 - \sum_{i=1}^{N} x_i)$ to (2.32) and varying with respect to x_i we obtain

$$\partial_i F_\lambda = T \ln x_i - NT_0 x_i - B_i - \lambda = 0 \ , \qquad i = 1, 2, \ldots, N \ . \tag{2.34}$$

The Lagrange multiplier λ can be eliminated by subtracting one of the relations, say for $i = N$, from the rest (which is equivalent to solving the constraint and expressing one of the x_i, say x_N, in terms of the others). We obtain

$$T \ln \frac{x_i}{x_N} - NT_0(x_i - x_N) - (B_i - B_N) = 0 \ , \quad i = 1, 2, \ldots, N-1 \ , \tag{2.35}$$

where x_N is determined from the constraint (2.31). Also, from (2.34) we obtain the second derivatives

$$\partial_i \partial_j F_\lambda = \Big(\frac{T}{x_i} - NT_0 \Big) \delta_{ij} \ , \quad i, j = 1, 2, \ldots, N \ , \tag{2.36}$$

subject to (2.31). The above Hessian will be needed later in order to investigate the stability of the solutions. The simpler form of the equations (2.34) involving λ will also be useful in determining the nature of solutions and in the stability analysis.

3. Phase transitions with vanishing magnetic fields

We now put $B_i = 0$ (setting all of the B_i equal is equivalent, as this would be a $U(1)$ field and would contribute a trivial constant to the energy) and examine the phase structure of the system. We can collectively write equations (2.34) for $B_i = 0$ as

$$T \ln x - NT_0 x = \lambda \ , \tag{3.1}$$

dropping the index i in x_i to emphasize that it is the same equation for all x_i's, unlike the case with generic non-vanishing magnetic fields. The value of λ is fixed by the summation condition (2.31).

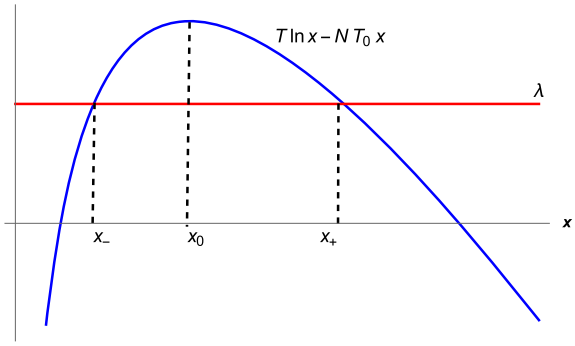

Fig. 1. Plot of the LHS of (3.1), with its maximum occurring at $x_0 = \frac{T}{NT_0}$. The intersection with some constant value of the Lagrange multiplier λ occurs at $x = x_\pm$, with $x_- < x_0 < x_+$.

We note that (3.1) always admits the trivial solution $x_i = 1/N$ (for an appropriate λ), corresponding to the singlet irrep and an unbroken $SU(N)$ phase. Generically, however, the above equation has two solutions (see Fig. 1). So, each x_i can have one of two fixed values, x_- or $x_+ > x_-$. This means that the dominant irreps are those with M equal rows, where M is the number of x_i having the large stvalue x_+ in the solution, and gives $SU(M) \times SU(N-M) \times U(1)$ as the possible *a priori* spontaneous breaking of $SU(N)$, the subgroup that preserves a matrix with M equal and $N-M$ different and equal diagonal entries. We will see, however, that stability of the configuration requires that at most one x_i value in the full solution be $x = x_+$; that is, either $M = 0$, corresponding to the singlet, or $M = 1$, corresponding to a one-row YT, a completely symmetric representation.

Then equations (2.35) with $B_i = 0$ become

$$T \ln \frac{x_i}{x_N} = NT_0(x_i - x_N) \ , \quad i = 1, 2, \ldots, N-1 \ , \tag{3.2}$$

where $x_N = 1 - x_1 - \cdots - x_{N-1}$ is determined by the constraint in (2.31).

As argued before from (3.1), each x_i can have one of two possible values. Hence, take M of the x_i to be equal, and the remaining $N-M$ also equal and different. The integer M can take any value from 0 to N, but the values $M = 0$ and $M = N$ correspond to the singlet configuration $x_i = 1/N$ that trivially satisfies (3.1). For $M \neq 0, N$, taking into account the summation to one condition, we set

$$\begin{aligned} x_i &= \frac{1+x}{N} \ , \qquad i = 1, 2, \ldots, M \ , \\ x_i &= \frac{1-ax}{N} \ , \quad i = M+1, \ldots, N \ , \qquad a = \frac{M}{N-M} \ . \end{aligned} \tag{3.3}$$

Note that, according to (2.15), the x_i's cannot strictly be equal for finite n. However, in the large n limit, differences of $\mathcal{O}(1/n)$ are ignored. Further, the choice of the specific x_i that we set to each value is irrelevant, since the saddle point equations for $B_i = 0$ are invariant under permutations of the x_i. With the choice (3.3), $N-M$ of the equations are identically satisfied and the remaining M amount to

$$T \ln \frac{1+x}{1-ax} - (1+a)T_0 x = 0 \ . \tag{3.4}$$

This transcendental equation is invariant under the transformation

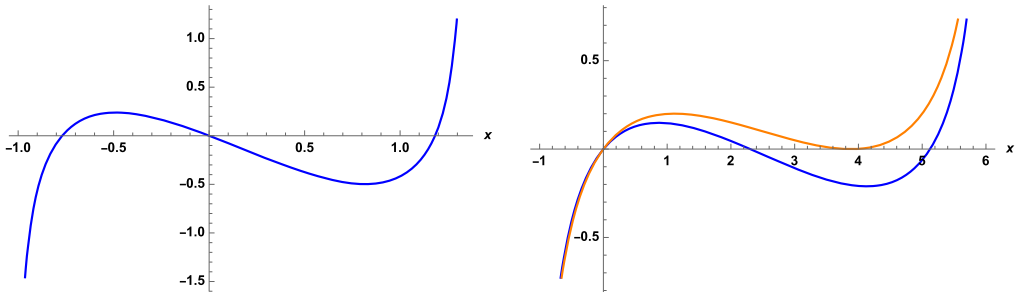

Fig. 2. Plots of the left hand side of (3.4) for $N = 7$. Left: $M = 3$, $T = 0.7$. Right: $M = 1$, $T = 1.6$ (blue) and for $T = T_c \simeq 1.72$ (corresponding to $x = x_c \simeq 3.88$) (orange). Temperature is in units of T_0.

$$x \to -ax\ , \quad a \to 1/a \ \ \text{(equivalently } M \to N - M\text{)}\ . \tag{3.5}$$

Thus, without loss of generality we can choose

$$M \leqslant [N/2]\ , \quad \text{or} \quad 0 < a \leqslant 1\ , \quad x \in (-1, 1/a)\ , \tag{3.6}$$

where $[\,\cdot\,]$ denotes the integer part. Solutions with $x > 0$ specify an irrep with M equal rows of length, using (2.16) and (3.3),

$$\ell_i = \frac{x}{N-M}\, n + \mathcal{O}(1)\ , \quad i = 1, \ldots, M\ , \qquad \ell_i = \mathcal{O}(1)\ , \quad i = M+1, \ldots, N-1\ . \tag{3.7}$$

Instead, an $x < 0$ specifies an irrep with $N - M$ equal rows (corresponding to the conjugate representation), with length given by (3.7) but with x replaced by $x \to -x$. The reason is that in this case the x_i's in the second line of (3.3) are larger than those of the first line and therefore the roles of M and $N - M$ are reversed.

There are generically either one or three solutions to (3.4) depending on T (see Fig. 2). If the temperature is higher than a critical temperature T_c, then the only solution is that with $x = 0$, that is, the singlet. If $T < T_c$, then there are two additional solutions. For $T = T_c$ these two solutions coalesce at $x = x_c$, implying that the x-derivate of (3.4) is zero as well at x_c. These conditions are summarized as

$$\begin{aligned} &\frac{T_c}{T_0} \ln \frac{1 + x_c}{1 - a x_c} = (1 + a) x_c\ , \\ &(1 + x_c)(1 - a x_c) = \frac{T_c}{T_0} \equiv t\ . \end{aligned} \tag{3.8}$$

Solving the first condition for $t = T_c/T_0$ and substituting into the second we obtain a transcendental equation that determines x_c

$$\frac{(1 + a) x_c}{(1 + x_c)(1 - a x_c)} = \ln \frac{1 + x_c}{1 - a x_c} \tag{3.9}$$

and from that and the first of (3.8) the critical temperature T_c. Alternatively, solving the second equation in (3.8) for x_c and substituting into the first one yields the transcendental equation for $t = T/T_0$

$$\ln\left(\frac{1}{a}\frac{1 + a + \sqrt{(1+a)^2 - 4at}}{1 + a - \sqrt{(1+a)^2 - 4at}}\right) - \frac{1 + a}{2at}\left(1 - a + \sqrt{(1+a)^2 - 4at}\right) = 0\ , \tag{3.10}$$

which assumes that $a \leqslant 1$. For $a \geqslant 1$ we simply replace $a \to 1/a$.

For $SU(2)$, $a = 1$ is the only possibility, and for $a = 1$ the solution of (3.10) is $t = 1$. Hence, the critical temperature is just T_0, i.e. the one in (2.33). For generic a, it can be checked that the left hand side of (3.10) is monotonically increasing in t and the equation has a unique solution in the range $1 < t < \frac{(1+a)^2}{4a}$ for all $a \leqslant 1$. For a near 1 we have

$$t = 1 + \frac{1}{6}(1-a)^2 + \dots \,, \tag{3.11}$$

whereas for a near 0

$$\frac{1}{t} = a\big(-\ln a + \ln(-\ln a)\big) + \dots \tag{3.12}$$

and therefore $t \to \infty$. Hence, the solution to (3.10) varies monotonically between these two limiting cases. Note that for the case $M = 1$, $a = 1/(N-1)$ (which is particularly relevant, as we shall see)

$$M = 1: \qquad T_c \simeq T_0 \frac{N}{\ln N} \gg T_0 \,, \quad \text{as} \quad N \gg 1 \,. \tag{3.13}$$

In conclusion, $T_c > T_0$ for any group $SU(N)$ with $N \geqslant 3$. For $T > T_c$ the only solution is the trivial one, $x = 0$, while for $T < T_c$ there are two additional solutions x_1, x_2: two positive ones $0 < x_1 < x_c < x_2$ for $T_0 < T < T_c$, and one positive and one negative one $x_1 < 0 < x_2$ for $T < T_0$. A few generic cases are depicted in Fig. 1 where the left hand side of (3.4) is plotted.

3.1. Stability analysis and critical temperatures

The solutions of (3.4) may be local extrema or saddle points of the action. To determine their stability we examine the second variation of the free energy. From (2.36), $\delta^2 F$ is

$$\delta^2 F = \frac{1}{2}\sum_{i=1}^{N} C_i^{-1} \delta x_i^2 \,, \qquad C_i^{-1} = \frac{T}{x_i} - NT_0 \,, \qquad \sum_{i=1}^{N} \delta x_i = 0 \,. \tag{3.14}$$

Note that this remains the same even in the presence of magnetic fields, so the stability argument below is fully general.

If all coefficients C_i are positive at a stationary point, then clearly the solution is stable. If two or more C_i's are negative, on the other hand, it is unstable. Indeed, we can take, e.g., $\delta x_{i_1} + \delta x_{i_2} = 0$ for two of the negative coefficients C_{i_1} and C_{i_2}, and set the rest of the δx_i to zero in order to satisfy the constraint. Then, an obvious instability arises. However, if only *one* C_i is negative and the rest of them positive, then the solution could still be stable due to the presence of the constraint. A standard analysis shows that the condition for stability in this case is[2]

$$\sum_{i=1}^{N} C_i < 0 \,. \tag{3.15}$$

[2] A nice way to derive this is to view δx_i as covariant coordinates on a space with metric $g_{ij} = C_i \delta_{ij}$ of Minkowski signature $(-,+,\dots,+)$. Then $\delta^2 F$ and the constraint become

$$\delta^2 F = g^{ij}\delta x_i \delta x_j \,, \quad u^i \delta x_i = 0 \quad \text{with} \quad u^i = 1 \,.$$

For the space spanned by the restricted δx_i to be spacelike (with positive definite metric), u_i must be timelike, and $u^i u_i = g_{ij} u^i u^j < 0$ implies (3.15).

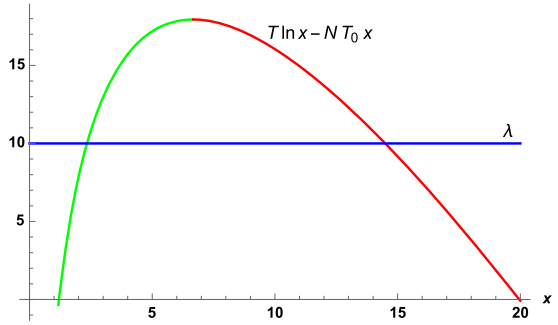

Fig. 3. Plot of (3.16), with its maximum occurring at $x_0 = \frac{T}{NT_0}$. The intersection with some constant value of the Lagrange multiplier λ occurs at the values $x_i = x_\pm$, with $x_- < x_0 < x_+$. The left (green) part of the curve corresponds to stable solutions, whereas the right one (red) to unstable ones.

For the case of vanishing magnetic field, x_i satisfy the common equation (3.1)

$$T \ln x - NT_0 x = \lambda \ . \tag{3.16}$$

The function on the left hand side is plotted in Fig. 1, repeated here as Fig. 3, and has a maximum at $x_0 = \frac{T}{NT_0}$ for all i. For $x = x_0$, the coefficient C_i^{-1} determining the perturbative stability at this value vanishes, while $C_i^{-1} > 0$ for $x < x_0$ and $C_i^{-1} < 0$ for $> x_0$. Therefore, the left branch of the curve represents *a priori* stable points and the right branch unstable ones.

From the above general discussion, we understand that fully stable configurations correspond either to choosing all x_i's on the stable branch (all $C_i > 0$), or $N-1$ of them on the stable branch and one on the unstable branch (only one $C_i < 0$). This last configuration can still be stable if it satisfies the condition (3.15). So the only potentially stable configurations for zero magnetic field are the singlet ($M = 0$), corresponding to a paramagnetic phase, and the fully symmetric single-row irrep ($M = 1$), corresponding to a specific ferromagnetic phase, with order parameter the variable x in (3.3) determining the length of the single row.

For the remainder of the zero magnetic field discussion we will focus on the nontrivial solution $M = 1$ and set for the constant $a = M/(N-M)$ the corresponding value

$$a = \frac{1}{N-1} \ . \tag{3.17}$$

For this choice, and with x_i as in (3.3), the coefficients C_i become

$$C_1^{-1} = N\, A(x) \ , \qquad C_i^{-1} = N\, A(-ax) \ , \quad i = 2, 3, \ldots, N \ , \tag{3.18}$$

where we defined

$$A(x) = \frac{T}{1+x} - T_0 \ . \tag{3.19}$$

The stability of the no magnetization solution $x = 0$ corresponding to the singlet is easy to find. In that case $A(0) = T - T_0$, so that for $T < T_0$ the solution $x = 0$ is a local maximum and unstable, and for $T > T_0$ it is a local minimum.

For $M = 1$, it is clear from Fig. 3 that we must have $C_1 < 0$, corresponding to the single value $x_1 = (1+x)/N$ on the unstable branch, and the remaining $C_i > 0$, so $A(x) < 0$ and $A(-ax) > 0$. Also, $1 + x > 1 - ax$, so that $x > 0$. Condition (3.15) must also be satisfied,

$$A(x) + aA(-ax) > 0 \quad \Longrightarrow \quad (1+x)(1-ax) < \frac{T}{T_0} \,, \tag{3.20}$$

where we used $N - 1 = a^{-1}$. Using (3.4) to eliminate T this rewrites as

$$\frac{(1+a)x}{(1+x)(1-ax)} > \ln \frac{1+x}{1-ax} \,. \tag{3.21}$$

Note that this has the same form as (3.9) determining the critical x_c. It can be seen that it is satisfied for $x > x_c$ and violated for $x < x_c$.

As analyzed in the previous section, the existence of solutions with $M = 1$ requires $T < T_c$. For such temperatures, equation (3.4) has two solutions, one larger and one smaller than x_c. Only the solution with $x > x_c$ satisfies (3.21). Therefore, for temperatures $T < T_c$ the solution with $x > x_c$ is stable and a local minimum and the one with $x < x_c$ unstable. Referring again to Fig. 2, the solution to the left of $x = x_c$ for $T < T_c$ (blue) on the right plot is unstable, whereas the one to the right is stable.

We conclude by noting that at low temperatures $T \ll T_0$, we expect the stable configuration of the system to be the fully polarized one with $x \simeq x_{\max} = N - 1$, corresponding to the maximal one-row symmetric representation with $\ell_1 \simeq n$ boxes. Indeed, the solution of equation (3.4) in that case can by well approximated by

$$x \simeq (N-1)\Big(1 - Ne^{-NT_0/T}\Big) \,, \qquad T \ll NT_0 \,, \tag{3.22}$$

manifesting a nonperturbative behavior in T around $T = 0$.

3.2. Phase transitions and metastability

We saw in the previous section that for $T_0 < T < T_c$ both the completely symmetric representation and the singlet are locally stable. The globally stable configuration is determined by comparing the free energies of the two solutions. The free energy per atom was found in (2.32). For zero magnetic fields, it takes the form

$$F(\mathbf{x}, T) = \sum_{i=1}^{N} \Big(T x_i \ln x_i - \frac{NT_0}{2} x_i^2 \Big) \tag{3.23}$$

and for the single-row zero magnetic field solution the free energy per atom becomes

$$\begin{aligned} F_{\rm sym}(x, T) = & \frac{T}{1+a} \big(a(1+x)\ln(1+x) + (1-ax)\ln(1-ax) \big) \\ & - \frac{a}{2} T_0 x^2 - T \ln N \,. \end{aligned} \tag{3.24}$$

Variation of this expression with respect to x leads to (3.4).[3] For the singlet we have

$$F_{\rm singlet}(T) = -T \ln N \,. \tag{3.25}$$

[3] Positivity of the second derivative gives the stability condition (3.20), but without any restriction on a, that is, the number M of equal rows in the YT. The reason is that this expression only captures stability under variations of the length of the YT. Taking also into account perturbations into configurations with additional rows recovers the general stability condition requiring $M = 0$ or $M = 1$.

Table 1
Phases in various temperature ranges for $N \geqslant 3$ and their stability characterization.

irrep	$T < T_0$	$T_0 < T < T_1$	$T_1 < T < T_c$	$T_c < T$
Singlet	unstable	metastable	stable	stable
Symmetric	stable	stable	metastable	not a solution

For a specific temperature T_1 and magnetization x_1 the singlet and symmetric configurations will have the same free energy. Equating the two expressions and using (3.4) we obtain

$$\begin{aligned} T_1 \ln \frac{1+x_1}{1-ax_1} &= (1+a)T_0 x_1 \ , \\ T_1 \ln(1+x_1) &= \frac{T_0}{2} x_1(2-ax_1) \ , \end{aligned} \tag{3.26}$$

where we used (3.4) to simplify the expression for $F_{\rm sym}$. This system is solved by[4]

$$T_1 = \frac{T_0}{2} \frac{N(N-2)}{(N-1)\ln(N-1)} \ , \qquad x_1 = N-2 \ . \tag{3.27}$$

In general

$$T_0 < T_1 < T_c \ , \tag{3.28}$$

except for $N = 2$ where we have $T_0 = T_1 = T_c$, implying that for the $SU(2)$ case there is a single critical temperature. For large N

$$T_1 \simeq T_0 \frac{N}{2\ln N} \gg T_0 \ , \quad \text{as} \quad N \gg 1 \ . \tag{3.29}$$

Recalling the limiting behavior of T_c in (3.13), we note that for large N, $T_1 \simeq T_c/2$. For $T_0 < T < T_1$, $F_{\rm singlet} > F_{\rm sym}$, while for $T_1 < T < T_c$, $F_{\rm singlet} < F_{\rm sym}$. The situation is summarized in Table 1.

Hence, at high enough temperature the only solution is the singlet with no magnetization. At temperature T_c a magnetized state corresponding to the symmetric irrep (one-row) also emerges, and is metastable until some lower temperature T_1. Between these two temperatures the singlet is the stable solution. Below T_1 and down to T_0 the roles of stable and unstable solutions are interchanged. Below T_0 the only stable solution is the one-row symmetric representation. Hence, we have a spontaneous symmetry breaking as

$$SU(N) \to SU(N-1) \times U(1) \ . \tag{3.30}$$

Note that the free energy changes discontinuously at $T = T_0$ and at $T = T_c$. The plot of the free energy is at Fig. 4. The low temperature plateaux in Fig. 4 for the one-row configuration (blue curve) is explained by the fact that due to (3.22) we have

$$F_{\rm sym} \simeq -\frac{N-1}{2} T_0 \Big(1 + 2\frac{T}{T_0} e^{-NT_0/T}\Big) \ , \qquad T \ll NT_0 \ . \tag{3.31}$$

[4] In the next section we will present a method for solving it even in the presence of a magnetic field.

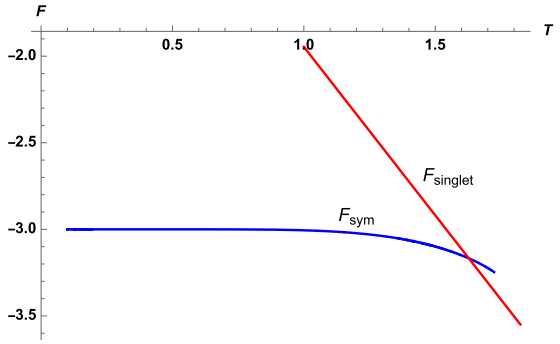

Fig. 4. Plot of the free energy F for $N = 7$, for the one-row solution (blue) up to $T_c \simeq 1.72$ and for the singlet one (red) from $T = 1$, in units of T_0. These cover the temperature range in which we have stability or metastability. The crossover behavior is at $T = T_1 \simeq 1.63$, in agreement with Table 1.

To better understand the situation, we may use the thermodynamic relations between the free energy F, the internal energy U and the entropy S

$$F = U - TS\,, \qquad U = -T^2\partial_T\left(\frac{F}{T}\right), \qquad S = -\partial_T F\,, \tag{3.32}$$

for $F_{\rm sym}$ given by (3.24) to obtain

$$\begin{aligned} U_{\rm sym}(x) &= -\frac{a}{2}T_0\,x^2\,,\\ S_{\rm sym}(x) &= \ln N - \frac{1}{1+a}\big(a(1+x)\ln(1+x) + (1-ax)\ln(1-ax)\big)\,. \end{aligned} \tag{3.33}$$

These are readily recognized as the coupling energy and the logarithm of the number of states per atom for representations close to the dominant symmetric one (we emphasize that $x = x(T)$ via (3.4)). For the singlet ($x = 0$) we simply have

$$U_{\rm singlet} = 0\,, \qquad S_{\rm singlet} = \ln N\,, \tag{3.34}$$

that is, the maximal energy and maximal entropy.

Even though the free energy is discontinuous at $T = T_c$, we may still think of the transitions at T_0 and T_c as a first order phase transitions, in the sense that the discontinuity of U implies that latent heat has to be transferred for the phase transition to occur. In detail we have

$$\begin{aligned} &T \to T_c^-: \qquad U_{\rm sym} = -\frac{T_0}{2(N-1)}x_c^2\,, \quad S_{\rm sym} = \ln N + \frac{x_c}{1+x_c} - \ln(1+x_c)\,,\\ &T \to T_c^+: \qquad U_{\rm singlet} = 0\,, \quad S_{\rm singlet} = \ln N\,, \end{aligned} \tag{3.35}$$

where we simplified $S_{\rm sym}$ by using relations (3.8). When we transition from below to above T_c, we must give energy to the system, which also increases its entropy (recall that, in the absence of volume effects, $dU = T\,dS$). The behavior of the energy and the entropy with temperature is depicted in Fig. 5.

At the intermediate temperature $T = T_1$, given in (3.27), there is the possibility of a first order phase transition from a metastable to a stable phase. Near that temperature

$$\begin{aligned} F_{\rm sym} &= -T\ln N + \frac{N-2}{N}\ln(N-1)\big(T - T_1\big) + \dots\,,\\ F_{\rm singlet} &= -T\ln N\,. \end{aligned} \tag{3.36}$$

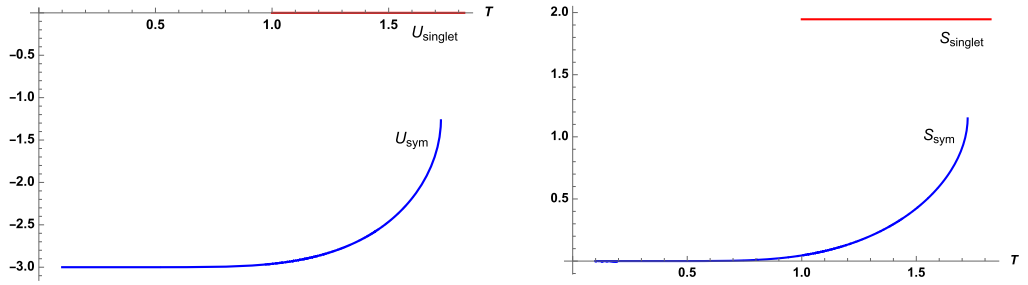

Fig. 5. Plots of U (left) and S (right) for $N = 7$. For the one-row solution (blue) up to $T_c \simeq 1.72$ and for the singlet one (red) from $T = 1$, in units of T_0. The sharp rise for $T \to T_c^-$ is according to (3.38).

This transition is typical in statistical physics where latent heat transfer is involved. Hence we have that

$$\begin{aligned} &T \to T_1^- : \qquad U_{\text{sym}} = -\frac{1}{2}\frac{(N-2)^2}{N-1}\,T_0\,, \quad S_{\text{sym}} = \ln N - \frac{N-2}{N}\ln(N-1)\,, \\ &T \to T_1^+ : \qquad U_{\text{singlet}} = 0\,, \quad S_{\text{singlet}} = \ln N\,. \end{aligned} \tag{3.37}$$

The transition from metastable to stable configurations near the temperature T_1 will not occur spontaneously under ideal conditions, leading to hysteresis. Only when the system is perturbed, or given an exponentially large time such that large thermal fluctuations occur, will it transition from a metastable to a stable configuration. This is reminiscent of the hysteresis in temperature exhibited in certain materials and in supercooled water [20]. The discontinuity in U implies that (latent) heat has to be transferred for the phase transition to occur. When we transit T_1 from above the system releases energy, which also lowers its entropy, the opposite happening when it transit above T_1 (the term "pseudo phase transition" has been used in the literature for this kind of process).

To understand the nature of the phase transitions that the system can undergo, imagine that we start at a temperature $T > T_c$ with the (paramagnetic) singlet state and adiabatically lower the temperature by bringing the system into contact with a cooling agent (reservoir). If the system is not perturbed, it will stay at the paramagnetic state until $T = T_0$, where this state becomes unstable, the (ferromagnetic) symmetric representation solution takes over, and the system undergoes a phase transition releasing latent heat into the reservoir. Similarly, starting at a temperature below T_0 with the (ferromagnetic) symmetric irrep state and raising adiabatically the temperature, the system will remain in this state if it is not perturbed and will transition to the singlet at $T = T_c$, absorbing latent heat from the reservoir and undergoing a phase transition. Clearly the system presents hysteresis, and no unique Curie temperature exists, since in the range $T_0 < T < T_c$ the two phases coexist.

The situation is somewhat different if the system is isolated (decoupled from the reservoir) while it is in a metastable state (that is, a ferromagnetic state at $T_1 < T < T_c$ or a paramagnetic state at $T_0 < T < T_1$). A transition to the stable state would involve exchange of latent heat, which can only be provided by, or absorbed into, the stable phase. However, the heat capacity of the paramagnetic phase is zero (see Fig. 5), so no such exchange can take place and the system is "trapped" in the unstable phase. This is unlike, say, supercooled water, where perturbations nucleate the formation of a stable solid state, releasing latent heat into the unstable liquid phase and raising the temperature until the liquid phase is eliminated or the temperature reaches the

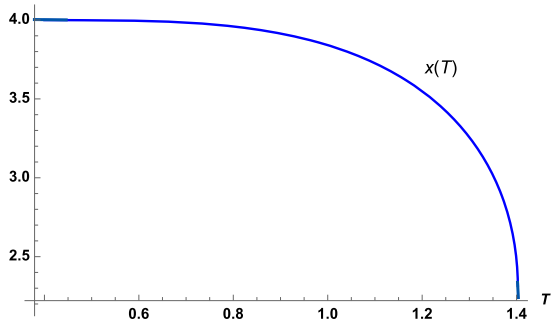

Fig. 6. Typical plot of $x(T)$ (here for $N = 5$) for the symmetric irrep for $0 < T < T_c \simeq 1.40$. For $T = 0$ it reaches the maximum value $x(0) = N - 1$ and for $T \to T_c^-$ it goes sharply to x_c according to (3.38).

point at which the two phases become equally stable. This feature of our system is somewhat unrealistic, since we have ignored all other degrees of freedom except $SU(N)$ spins. A realistic system would also have vibrational degrees of freedom of the atoms, which would serve as a reservoir absorbing or receiving latent heat and thus enabling transitions from metastable to stable states.

The parameter x is a measure of the spontaneous magnetization and constitutes the order parameter for the phase transition. Recalling (3.7), x is a measure of the length of the single row YT corresponding to the solution. From (3.4) and (3.8) we can deduce that $x(T)$ near T_c behaves as[5]

$$x - x_c \simeq \sqrt{\frac{(N-1)x_c}{x_c + 1 - N/2}} \sqrt{\frac{T_c - T}{T_0}} \,. \tag{3.38}$$

Hence, the deviation from x_c near the critical temperature follows Bloch's law for spontaneous magnetization of materials with an exponent of $1/2$ and an N-dependent coefficient. The behavior of $x(T)$ is depicted in Fig. 6.

The $SU(2)$ case: The above results are valid for $a \neq 1$ that is for $N \geqslant 3$. When $a = 1$, as in the $SU(2)$ case, $T_0 = T_1 = T_c$ and the stable-metastable range in Table 1 does not exist. The transition between the singlet and the symmetric representations occurs at the unique Curie temperature $T = T_0$ and at $x_c = 0$. In this case we have

$$\begin{aligned} &\text{Symm. irrep}\,(T < T_0)\text{:}\;\; x \simeq \sqrt{3}\sqrt{\frac{T_0 - T}{T_0}}\,, \quad F \simeq -T\ln 2 - \frac{3T_0}{4T_0}\big(T_0 - T\big)^2\,, \\ &\text{Singlet}\,(T > T_0)\text{:} \qquad x = 0\,, \quad F = -T\ln 2\,, \end{aligned} \tag{3.39}$$

which shows that at $T = T_0$ there is a second order phase transition.

Note that the naïve limit $a \to 1$ of the result (3.38) for $a < 1$ would not recover the above behavior. The reason is that the range of validity of (3.38) is $T_0 < T \lesssim T_c$, and it shrinks to zero as $T_c \to T_0$. The two first-order phase transition points at T_0 and T_c fuse into a single second-

[5] Positivity of $x_c + 1 - N/2$ follows from the fact that between the unstable and the stable solutions the left hand side of (3.4) as a function of x reaches a minimum (see the right plot in Fig. 2.

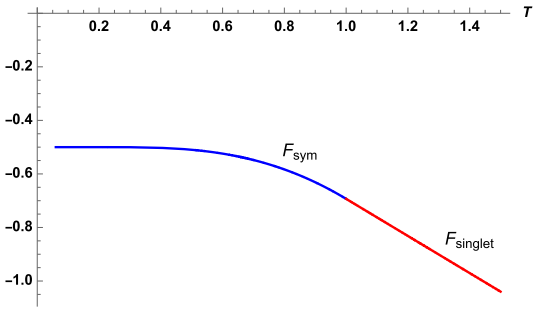

Fig. 7. Plot of the free F for $N = 2$. The continuity of the expression and its first derivative between the one-row solution (blue) up to $T = 1$ and the singlet one (red) from $T = 1$, in units of T_0, is manifest.

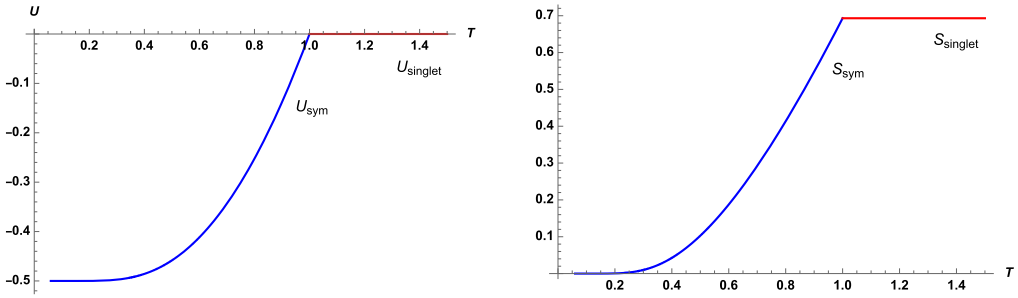

Fig. 8. Plots of U (left) and S (right) for $N = 2$ for T in units of T_0, for the magnetized (blue) state up to T_0 and the singlet (red) state above T_0.

Table 2
Behavior near critical point for $N = 2, 3, 4, 5$, as well as for $N \gg 1$ (the corresponding entries are leading).

N	2	3	4	5	$N \gg 1$
T_c/T_0	1	1.0926	1.2427	1.4027	$N/\ln N$
$x_c/x_{\max}$	0	0.3772	0.5071	0.5749	1
K	1.7320	1.2177	0.9862	0.8480	$\sqrt{2/N}$

order transition in the limit $a \to 1$. Fig. 7 depicts the free energy against the temperature for the $SU(2)$ case.

The behavior of $x(T)$ near $T = T_0$ follows Bloch's law with an exponent $1/2$, as in the general $SU(N)$ case, but with a different coefficient. The internal energy and entropy are continuous but their first derivatives at $T = T_0$ are not, as depicted in Fig. 8.

For comparison between $SU(2)$ and higher groups, we present in Table 2 the values of the critical temperature in units of T_0, the critical magnetization as a fraction of the maximal magnetization $x_{\max} = N - 1$ and the coefficient of $x - x_c$ in Bloch's law in (3.38) again as a fraction of the maximal magnetization, i.e. $K = \sqrt{(N-1)x_c/(x_c + 1 - N/2)}/x_{\max}$ for the first few values of N, as well as for $N \gg 1$.

4. Turning on magnetic fields

We now turn to incorporating nonzero magnetic fields in the system. We recall the equilibrium equation (2.34)

$$T \ln x_i - N T_0 x_i = B_i + \lambda \,, \qquad i = 1, 2, \ldots, N \,, \tag{4.1}$$

where the x_i sum to 1 due to the constraint in (2.31).

4.1. Small fields

For small magnetic fields the solution of the coupled equations (4.1) can be found as a perturbation of the solution for vanishing fields. In fact, we can do better than that. We may consider the response of the system in the presence of generic magnetic fields B_i under small perturbations δB_i. The state will change as

$$x_i \to x_i + \delta x_i \,, \quad i = 1, 2, \ldots, N \,, \tag{4.2}$$

where δx_i is a perturbation to the solution of (4.1). To linear order we have that

$$\left(\frac{T}{x_i} - N T_0 \right) \delta x_i = C_i^{-1} \delta x_i = \delta B_i + \delta\lambda \,. \tag{4.3}$$

Since $\sum_{i=1}^{N} \delta x_i = 0$ we obtain the change of λ as

$$\delta\lambda = - \frac{\sum_{i=1}^{N} C_j \delta B_j}{\sum_{i=1}^{N} C_j} \,. \tag{4.4}$$

Then, combining with (4.3) we get

$$\delta x_i = C_i \left(\delta B_i - \frac{\sum_{j=1}^{N} C_j \delta B_j}{\sum_{j=1}^{N} C_j} \right) , \tag{4.5}$$

from which the magnetizability matrix m_{ij} obtains as

$$m_{ij} = \frac{\partial x_i}{\partial B_j} = C_i \, \delta_{ij} - \frac{C_i C_j}{\sum_{k=1}^{N} C_k} \,, \qquad i, j = 1, 2, \ldots, N \,. \tag{4.6}$$

Note that m_{ij} is symmetric and satisfies $\sum_{i=1}^{N} m_{ij} = 0$ as a consequence of the fact that the $U(1)$ part decouples.

We may infer the signs of m_{ij} for general C_i's from the stability condition on the configuration. Recall that, for stability, either all C_i are positive (including infinity), or only one of them is negative, say C_1, and the rest positive (x_1 is the largest among the x_i's). In the latter case, stability further requires that (3.15) be satisfied. Using these we can show that

$$\begin{aligned}
C_1 > 0 : &\qquad m_{11}, m_{ii} > 0 \,, \quad m_{1i} < 0 \,, \quad m_{ij} < 0 \,, \\
C_1 < 0 : &\qquad m_{11}, m_{ii} > 0 \,, \quad m_{1i} < 0 \,, \quad m_{ij} > 0 \,, \\
C_1^{-1} = 0 : &\qquad m_{11}, m_{ii} > 0 \,, \quad m_{1i} < 0 \,, \quad m_{ij} = 0 \,,
\end{aligned} \tag{4.7}$$

where $i, j = 2, 3, \ldots, N$ and $i \neq j$. According to (3.14), the last case above happens for $T = NT_0x_1$, which is possible only for $T < NT_0$, and corresponds to one of the solutions of (4.1) reaching the top of the function in the LHS of (3.1), depicted in Fig. 1.

4.1.1. The singlet

For the unmagnetized singlet configuration, stable for temperatures $T > T_0$, $x_i = 1/N$ and $C_i^{-1} = N(T - T_0)$. The magnetizability is

$$\text{singlet}: \quad m_{ij} = \frac{1}{N(T-T_0)}\left(\delta_{ij} - \frac{1}{N}\right). \tag{4.8}$$

As expected, it diverges as $(T - T_0)^{-1}$ at the critical temperature T_0 where the configuration destabilizes, and the signs of its components are in agreement with (4.7). This determines the linear response of the system to small magnetic fields, of typical magnitude B such that $B \ll T - T_0$.

4.1.2. The symmetric representation

For the spontaneously magnetized configuration corresponding to the symmetric representation $M = 1$, stable for $T < T_c$, the x_i are as in (3.3), with x the solution of (3.4) that corresponds to a stable configuration. The components of the magnetization matrix take the form

$$\begin{aligned} m_{11} &= \frac{N-1}{N\Delta(x)}\,, \\ m_{1i} &= -\frac{1}{N\Delta(x)}\,, \quad i \neq 1, \\ m_{ij} &= \frac{1}{NA(-ax)}\left(\delta_{ij} - \frac{A(x)}{\Delta(x)}\right), \quad i, j \neq 1\,, \end{aligned} \tag{4.9}$$

where $a = 1/(N-1)$ and $A(x) = T/(1+x) - T_0$ as before, and

$$\Delta(x) = A(-ax) + \frac{1}{a}A(x) = N\left[\frac{T}{(1+x)(1-ax)} - T_0\right]. \tag{4.10}$$

As $T \to T_c^-$, (3.8) shows that the magnetization diverges. To compute its asymptotic behavior at $T \simeq T_c$ we use (3.38) to obtain

$$(1+x)(1-ax) = \frac{T_c}{T_0} - \sqrt{2x_c(2ax_c + a - 1)}\sqrt{\frac{T_c - T}{T_0}} + \ldots\,, \tag{4.11}$$

which implies

$$\Delta = N\frac{T_0}{T_c}\sqrt{2x_c(2ax_c + a - 1)}\sqrt{\frac{T_c - T}{T_0}} + \ldots\,. \tag{4.12}$$

Hence the entries of the magnetizability matrix as $T \to T_c^-$ become

$$\begin{aligned} m_{11} &\simeq \frac{N-1}{N^2}\frac{Q}{\sqrt{T_c - T}}\,, \\ m_{1i} &\simeq -\frac{1}{N^2}\frac{Q}{\sqrt{T_c - T}}\,, \\ m_{ij} &\simeq \frac{1}{N^2(N-1)}\frac{Q}{\sqrt{T_c - T}}\,, \quad i, j = 2, \ldots, N\,, \end{aligned} \tag{4.13}$$

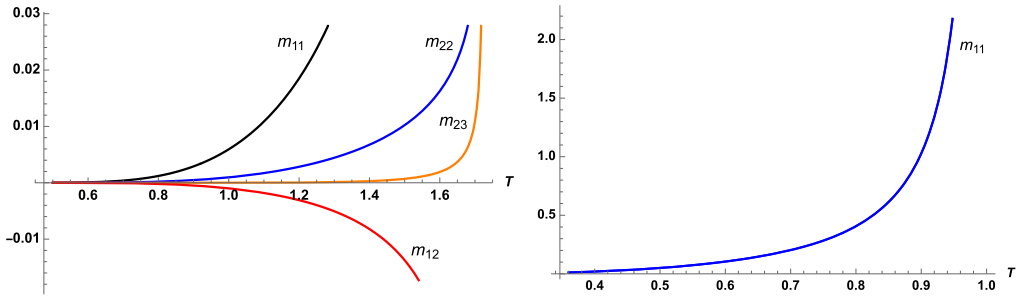

Fig. 9. Left: Plots of the four different types of magnetization matrix entries for the symmetric irrep. up to $T = T_c$ for $N \geqslant 3$. Right: Same plot for $SU(2)$.

where

$$Q = \frac{T_c/T_0}{\sqrt{2x_c(2ax_c + a - 1)T_0}} \,. \tag{4.14}$$

So the magnetizability diverges as $(T_c - T)^{-1/2}$, and the signs of its components are in agreement with (4.7). We have depicted these in Fig. 9 above.

The $SU(2)$ case: This is special since $T_c = T_0$. For the singlet solution ($T > T_0$), (4.8) remains valid for $N = 2$, giving

$$m_{11} = m_{22} = -m_{12} = \frac{1}{4}\frac{1}{T - T_0} \,, \qquad T \to T_0^+ \,. \tag{4.15}$$

For the magnetized solution

$$m_{11} = m_{22} = -m_{12} = \frac{1}{4}\frac{1 - x^2}{T - T_0(1 - x^2)} \,, \qquad T < T_0 \,. \tag{4.16}$$

Using (3.39) we obtain the magnetizability

$$m_{11} = m_{22} = -m_{12} \simeq \frac{1}{8}\frac{1}{T_0 - T} \,, \qquad T \to T_0^- \,. \tag{4.17}$$

We note that m_{ij} diverges as $|T - T_0|^{-1}$ on both sides of the critical temperature, unlike for $N \geqslant 2$. The reason is that the coefficient of $\sqrt{T_c - T_0}$ in the expansion (4.11) vanishes for $N = 2$ and thus the next order in the expansion, $\mathcal{O}(T_0 - T)$, becomes the leading one. We have depicted these in Fig. 9.

4.2. *Finite fields*

We now consider the state of the system, given by (4.1), for general non-vanishing magnetic fields.

The general qualitative picture can be obtained by the same considerations as in the case of $B_i = 0$. For fixed λ, each x_i satisfies (4.1) for a different effective Lagrange multiplier $\lambda_i = \lambda + B_i$ and can take two possible values $x_{i\pm}$, the two solutions of (4.1) for fixed i. The stability considerations of section 3.1, which remain valid for arbitrary magnetic fields, determine that at most one of these solutions can lie on the unstable branch of the curve x_+. So, fully stable

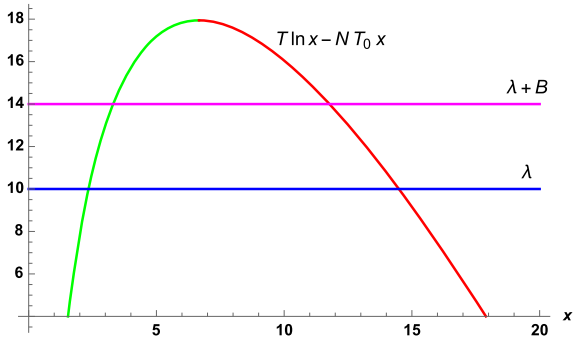

Fig. 10. Plot of (3.16), with its maximum occurring at $x_0 = \dfrac{T}{NT_0}$. We consider a magnetic field B along one direction, say for $i = 1$. The intersection with the lines λ and $\lambda + B$ occur at two values of x^i on each side of x_0 for each line.

configurations correspond either to choosing all x_{i-} on the stable branch, or $N-1$ of them on the stable branch and one on the unstable branch. The stability condition $\sum_i C_i < 0$ in (3.15) must also be satisfied in the latter case.

To gain intuition on the behavior of the system, we focus on the case when only one of the magnetic fields, say B_1, is different from the rest. We can absorb the equal terms B_i, $i > 1$ in the Lagrange multiplier and call $B = B_1 - B_i$. Then the set of equations (4.1) becomes just two distinct equations: one for x_1, with RHS $\lambda + B$, and one for the remaining $N-1$ x_i's, with RHS λ, as depicted in Fig. 10.

Referring to Fig. 10, denote the four solutions of (4.1) by $x_\pm$ (at the intersections of the curve with λ), and by $x_\pm^B$ (at the intersections with $\lambda + B$). For the choice of $B > 0$ in the figure we have the ordering $x_- < x_-^B < x_0 < x_+^B < x_+$. For $B < 0$ the ordering would change to $x_-^B < x_- < x_0 < x_+ < x_+^B$. Since we have a magnetic field only in direction 1, x_1 can take values $x_\pm^B$ while each x_i ($i > 1$) can take values $x_\pm$.

For a stable configuration we may choose at most one value at x_+ or x_+^B. Thus, we have the following possible cases:

- a) $N-1$ values x_- and one value x_-^B, corresponding to a one-row YT (if $x_-^B > x_-$) or its conjugate (if $x_-^B < x_-$). This is the deformation of the singlet for $B = 0$.
- b) $N-1$ values x_- and one value x_+^B, corresponding, again, to a one-row YT. This is the deformation of the one-row solution for $B = 0$.
- c) $N-2$ values x_-, one value x_-^B, and one value x_+, corresponding to a two-row YT. This is a deformation of the one-row YT solution at $B = 0$ by increasing its depth and breaking the $SU(N)$ symmetry further. Following a similar analysis, these would correspond either to irreps with two rows, or to irreps with $N-1$ rows, $N-2$ of which have equal lengths. We will encounter such cases below.

Although we will not examine in detail the more general configuration of a magnetic field with M equal components and the remaining $N-M$ equal and distinct, its qualitative analysis is similar. Fig. 10 remains valid, but now with M values of x_i at $\lambda + B$ and $N-M$ at λ. Implementing the stability criterion we have the following cases (for $B > 0$):

- $N-M$ values x_- and M values $x_-^{B_i}$, corresponding to a YT with M rows. This is the deformation of the singlet for $B=0$.
- $N-M$ values x_-, $M-1$ values $x_-^{B_i}$, and one value $x_+^{B_i}$, corresponding to a YT with M rows. This is the deformation of the one-row solution for $B=0$.
- $N-M-1$ values x_-, M values $x_-^{B_i}$, and one value x_+, corresponding to a YT with $M+1$ rows. This is the deformation of the one-row solution for $B=0$ by increasing its depth and breaking the $SU(N)$ symmetry further.

Overall, equality of magnetic field components results in states with equal rows in their YT.

4.2.1. One-row and conjugate one-row states

We proceed to investigate quantitatively the effect of a magnetic field in one direction (say, 1) in the case where the system is in a one-row solution in the same direction, or the corresponding conjugate representation. That is, we will examine the cases (a) and (b) above (case (c) will be examined in the next subsection). Then the equation for the system becomes[6]

$$T \ln \frac{1+x}{1-ax} = T_0\,(1+a)x + B\ , \qquad -1 < x < \frac{1}{a} = N-1\ . \tag{4.20}$$

Solutions to this equation with $x>0$ correspond to a single row YT, whereas solutions with $x<0$ to its conjugate, that is, a YT with $N-1$ rows of equal lengths. These are related by observing that (4.20) is invariant under $x\to -x/a$, $B\to -B$, and $a\to 1/a$, which maps symmetric irreps to their conjugate.

The stability conditions for the solution are determined by the general discussion in the previous subsection. As before, according to (3.18) $C_1^{-1} = NA(x)$, with $A(x)$ defined in (3.19), and thus $C_i^{-1} = NA(-ax)$ for $i>1$. By its definition, $A(x)$ satisfies

$$\begin{aligned} &x>0: \quad A(x) < A(-ax)\ , \\ &x<0: \quad A(x) > A(-ax)\ . \end{aligned} \tag{4.21}$$

The general stability argument requires $C_i>0$ for $i>1$, that is, $A(-ax)>0$. For $C_1<0$ we must also have $\sum_i C_i<0$, or $A(x)+aA(-ax)>0$, as it was shown in (3.15) and (3.20). Altogether, combined with (4.21), the stability conditions that cover all cases are

$$x>0: \quad A(x)+aA(-ax)>0\ , \tag{4.22}$$

which guarantees positivity of $A(-ax)$ no matter what the sign of $A(x)$, and

$$x<0: \quad A(-ax)>0\ . \tag{4.23}$$

[6] Note that for $a=1$ (the $SU(2)$ case) and after setting $x=\frac{T}{T_0}y-\frac{B}{2T_0}$ equation (4.20) becomes

$$y = \frac{B}{2T} + \frac{T_0}{T}\tanh y\ , \tag{4.18}$$

which is the standard expression in phenomenological investigations of ferromagnetism [21]. For $a\neq 1$ (the $SU(N)$ case with $N\geqslant 3$) this is modified by setting $x=\frac{2Ty-B}{(1+a)T_0}$ and results to the generalization

$$y = \frac{B}{2T} + \frac{T_0}{T}\frac{1}{\coth y - \frac{N-2}{N}}\ . \tag{4.19}$$

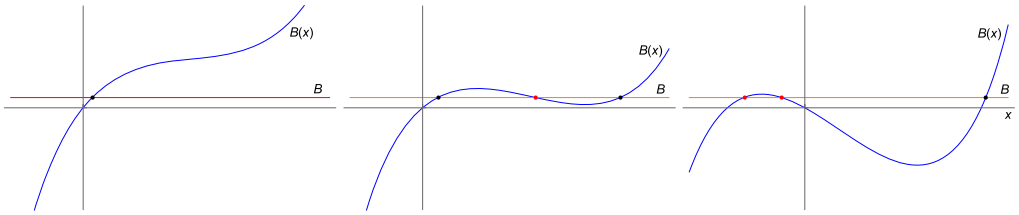

Fig. 11. Plot of $B(x)$ for $T > T_+$ (left), $T_0 < T < T_+$ (middle) and $T < T_0$ (right).

The condition (4.22) above will be satisfied for

$$x < x_- \text{ or } x > x_+ , \qquad x_\pm = \frac{N-2\pm\sqrt{N^2-4(N-1)T/T_0}}{2} , \tag{4.24}$$

while (4.23) will be satisfied for

$$x_0 < x < 0 , \qquad x_0 = (N-1)\left(1-\frac{T}{T_0}\right) . \tag{4.25}$$

The existence of $x_\pm$, and the condition that $x_0 > -1$, introduce two more temperatures

$$T_+ = \frac{N^2}{4(N-1)}T_0 > T_0 , \qquad T_- = \frac{N}{N-1}T_0 > T_0 . \tag{4.26}$$

For $T > T_+$, (4.22) is satisfied for all $x > 0$, while for $T > T_-$, (4.23) is satisfied for all $x < 0$. Note that both $x_\pm \in (-1, N-1)$, and that $x_+ > 0$, while $x_- > 0$ for $T > T_0$ and $x_- < 0$ for $T < T_0$. In terms of relative ordering of temperature scales,

$$\begin{aligned} &N = 3: \quad T_+ = \frac{9T_0}{8} < T_- = \frac{3T_0}{2} , \\ &N = 4: \quad T_+ = T_- = \frac{4T_0}{3} , \\ &N > 4: \quad T_+ > T_- . \end{aligned} \tag{4.27}$$

We proceed to the analysis of the states of the system. It is most convenient to keep x and T as the free variables and consider the magnetic field B as a function of x with T as a parameter. Then (4.20) implies

$$B(x) = T\ln\frac{1+x}{1-ax} - T_0(1+a)x . \tag{4.28}$$

Note that

$$\frac{dB}{dx} = \frac{a(1+a)T_0}{(1+x)(1-ax)}(x-x_+)(x-x_-) = T_0\big(A(x)+aA(-ax)\big) . \tag{4.29}$$

Hence, dB/dx is proportional to the stability condition (4.22) for $x > 0$. Therefore, $B(x)$ is an increasing function of x for $T > T_+$ and $T < T_-$, and a decreasing one for $x_- < x < x_+$, with x_- and x_+ as local maxima and minima. The function $B(x)$ is plotted in Fig. 11 for various values of the temperature. The intersection of these graphs with the horizontal at B determines the solutions for the configuration of the system.

The above allow us to determine the stability of solutions for various values of the temperature and magnetic field. We consider two cases, according to (4.22) and (4.23).

Positive x: The constraint (4.22) is relevant. Therefore, when $T > T_+$, all solutions with $x > 0$ are stable. For $T_0 < T < T_+$, stability singles out solutions with $0 < x < x_-$ and $x > x_+$. Finally, for $T < T_0$, since then $x_- < 0$, stability requires that $x > x_+$.
Negative x: The constraint (4.23) is now relevant, or equivalently $x > x_0$. Since $x < 0$, we conclude that no stable solutions exist for $x_0 > 0$, or $T < T_0$. For $x_0 < -1$, or $T > T_-$, all $x < 0$ solutions are stable. Finally, for intermediate temperatures $T_0 < T < T_-$, we have stability for $-1 < x_0 < x < 0$.

The above are tabulated in Table 3 below (we assume that $N > 4$ so that $T_+ > T_-$):

Table 3
Stable solutions for various ranges of T and x and for $N > 4$.

x	$T < T_0$	$T_0 < T < T_-$	$T_- < T < T_+$	$T_+ < T$
$x < 0$	none	$-1 < x_0 < x$	all	all
$x > 0$	$x > x_+$	$x < x_-$ & $x > x_+$	$x < x_-$ & $x > x_+$	all

We can now investigate the existence of stable solutions for the full range of values of the temperature and the magnetic field. The complete analysis is relegated to appendix A. The results are summarized in the temperature-magnetic field phase diagram of Fig. 12, presented for a generic value for $N > 4$. The phase diagram is qualitatively the same for $N = 3$ and $N = 4$, changing only for $N = 2$. The only difference is that, for $N = 4$, $T_+ = T_-$, while for $N = 3$ $T_+ < T_-$. This does not affect the general features of the diagram, simply shifting the critical point vertex (T_+, B_+) to the left of the bottom asymptote $T = T_-$, for $N = 3$, or on top of it, for $N = 4$.

Each region in the T–B plane depicted in the figure corresponds to a discrete phase of the system. Moving within these regions without crossing any of the critical lines interpolates continuously between configurations. In the connected regions C_1, C_2, and C_3 there is a unique one-row configuration at each point (T, B). In regions A and B inside the curvilinear triangle there are *two* locally stable configurations at each point, one absolutely stable and the other metastable, with the line separating A and B being the border of metastability where the two phases have equal free energy. In region D there are *no* stable one-row solutions, signifying that a two-row solution must exist there. The lines separating regions $C_{1,2,3}$ and the other regions are phase boundaries, the configuration changing discontinuously as we cross a boundary.

The dashed curve for $T_0 < T < NT_0$ represents configurations with $C_1 = \infty$, that is, $A(x) = 0$. This corresponds to points where $x_1 = (1 + x)/N$ reaches the top of the curve in Fig. 10, transiting from the unstable to the stable branch of the curve or vice versa. For such points, $x = T/T_0 - 1$, and (4.28) gives B on this curve as

$$B(T) = T \ln \frac{(N-1)T}{NT_0 - T} - \frac{N(T - T_0)}{N-1} \,. \tag{4.30}$$

Configurations to the left of this curve are in a "broken-like" $SU(N)$ phase, with one of the solutions of (4.1) in the unstable branch of the curve in Fig. 10, while those to the right of the curve are in an "unbroken-like" phase, with all solutions on the stable branch. For $B = 0$ these are the true spontaneously broken or unbroken phases of the system. A nonzero magnetic field breaks $SU(N)$ explicitly, and the dashed line represents a soft phase boundary, which must be crossed to transit between the two phases as we move on the T–B plane. The physical signature of crossing

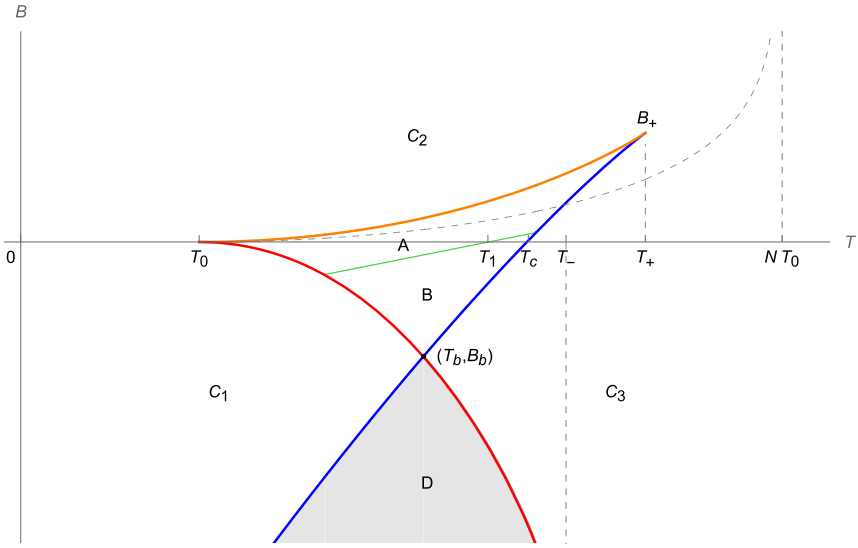

Fig. 12. The phase diagram of the system for generic $N > 4$. The (orange) curve separating regions A and C_2 is $B(x_-)$; the (blue) curve separating regions A, B, C_1 and C_3, D is $B(x_+)$, intersecting the T-axis at the $B = 0$ critical temperature $T = T_c$; and the (red) curve separating regions A, B, C_3 and C_1, D is $B(x_0)$ and it asymptotes to the vertical $T = T_-$. Crossing any of these lines precipitates a discontinuous change in the magnetization, i.e. the order parameter x. The (green) straight line separating regions A and B is the metastability frontier of the two coexisting phases inside these regions (see appendix A.1); crossing it exchanges the metastable and the absolutely stable states, and its intersection with the T-axis is the $B = 0$ critical temperature $T = T_1$. Regions $C_{1,2,3}$ constitute one continuous phase with nonzero magnetization (except at $B = 0$ and $T > T_c$), all points being accessible through continuous paths in the $B - T$ space, while regions A, B and D are separated from $C_{1,2,3}$ by discontinuous transitions in the order parameter. The (gray) dashed curve from T_0 to its vertical asymptote at $T = NT_0$ separates "broken-like" and "unbroken-like" configurations but otherwise mark no sharp phase transition. The shaded region D corresponds to a two-row (double magnetization) phase. For $N = 3$ the phase diagram remains qualitatively the same with the order of T_+ and T_- interchanged, while for $N = 4$, we simply have $T_+ = T_-$.

this boundary is that the off-diagonal elements of the magnetizability m_{ij}, with $i \neq j \neq 1$, change sign, vanishing on the boundary (see (4.7)).

The line separating regions B and C_3 intersects the T axis at the critical temperature T_c found in the $B = 0$ section. Points $(T_0, 0)$ and (T_+, B_+), with

$$B_+ = B(x_+(T_+)) = \frac{N}{2(N-1)}\left(\frac{N}{2}\ln(N-1) - N + 2\right), \tag{4.31}$$

are critical points, while point (T_b, B_b) at the lower tip of region B, satisfying the transcendental equation

$$B(x_0(T_b)) = B(x_+(T_b)) \equiv B_b \tag{4.32}$$

is a multiple critical point, connecting several different configurations: one one-row state in C_1, two in B, and one in C_3, as well as a two-row state in D, and possible two-row states in the other neighboring regions (see next section). One of the states in B, and possibly other one-row or two-row states, are metastable.

4.2.2. Two-row states and their $(N-1)$-row conjugates

As we have seen, for $T < T_-$ and for sufficiently negative magnetic fields there is no stable solution to (4.20), and thus no state corresponding to the one-row YT symmetric representation. From the general analysis of subsection 4.2, we expect the solution to be the only other allowed configuration, that is, a state corresponding to a two-row YT. In this subsection we recover this solution and check its stability.

We consider a configuration with two (generally unequal) lengths x_1 and x_2 and an applied magnetic field in the x_1-direction, representing the generic breaking pattern

$$SU(N) \to SU(N-2) \times U(1) \times U(1) \,, \tag{4.33}$$

of the $SU(N)$ symmetry. This includes a spontaneous breaking of $SU(N)$ in addition to the dynamical breaking $SU(N) \to SU(N-1) \times U(1)$ due to the magnetic field. We note that in the special case $x_1 = x_2$ the symmetry breaking pattern would be $SU(N) \to SU(N-2) \times SU(2) \times U(1)$, but as we shall demonstrate this pattern is never realized in the present case of a magnetic field in a single direction.

The x_i must satisfy the system of equations

$$\begin{aligned} T \ln \frac{x_1}{x_N} &= N T_0 (x_1 - x_N) + B \,, \\ T \ln \frac{x_i}{x_N} &= N T_0 (x_i - x_N) \,, \quad i = 2, 3, \ldots, N-1 \,, \end{aligned} \tag{4.34}$$

where x_N is determined from the constraint in (2.30). We write

$$\begin{aligned} x_1 &= \frac{1+x}{N} \,, \qquad x_2 = \frac{1+y}{N} \,, \\ x_3 &= \cdots = x_N = \frac{1-\alpha(x+y)}{N} \,, \quad \alpha = \frac{1}{N-2} \,. \end{aligned} \tag{4.35}$$

For $y = -\alpha x/(1+\alpha) = -ax = -x/(N-1)$ this ansatz reduces to the one for the one-row solution. (4.34) gives rise to the system of transcendental equations

$$\begin{aligned} T \ln \frac{1+x}{1-\alpha(x+y)} &= T_0\big(\alpha y + (1+\alpha)x\big) + B \,, \\ T \ln \frac{1+y}{1-\alpha(x+y)} &= T_0\big(\alpha x + (1+\alpha)y\big) \,. \end{aligned} \tag{4.36}$$

The free energy of the configuration is

$$\begin{aligned} F(x,y,T) = \frac{T_0}{2N(N-2)}\Big((x-y)^2 - N(x^2+y^2)\Big) + \frac{T}{N}\Big((1+x)\ln(1+x) \\ + (1+y)\ln(1+y) + (N-2-x-y)\ln\Big(1 - \frac{x+y}{N-2}\Big)\Big) - \frac{B}{N}x - T\ln N \,. \end{aligned} \tag{4.37}$$

The transcendental equations (4.36) will be solved numerically. The full analysis of solutions and their stability is relegated to the Appendix. Here we simply state the results and present relevant plots.

We consider temperatures $T < T_0$ for which spontaneous magnetization exists. As discussed earlier, for such temperatures and negative magnetic fields we expect the state to be in a two-row stable state, which includes the possibility of "antirows," that is, $N-2$ equal rows plus an

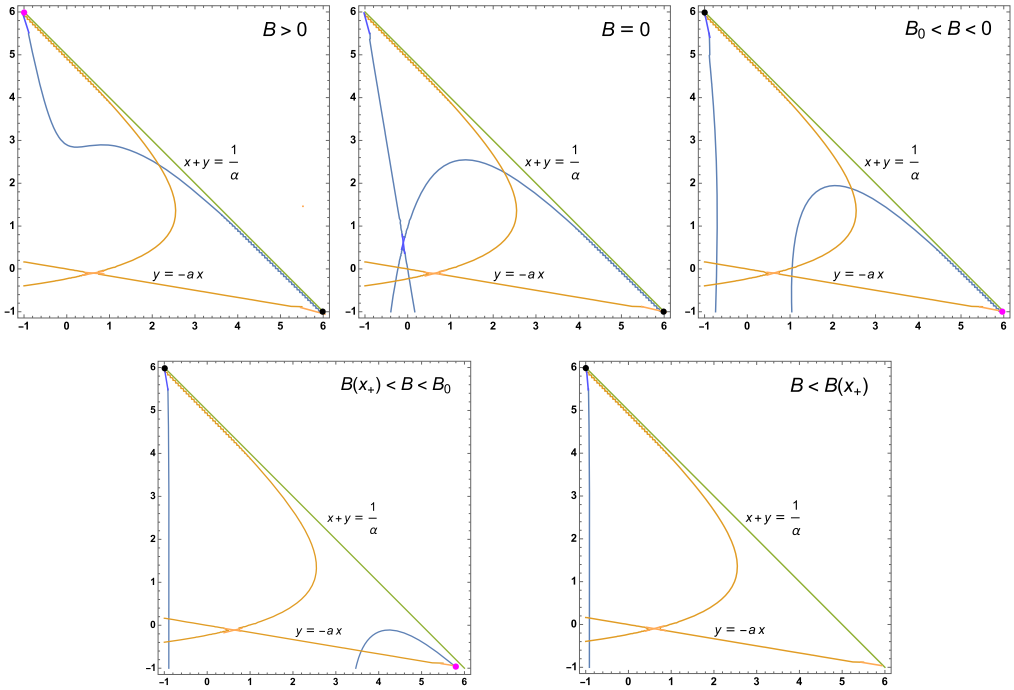

Fig. 13. Typical contour plots for $T < T_0$ in the $x-y$ plane of the two eqs. in (4.36), in blue (1st eq.) and orange (2nd eq., for which one of the branches is a straight line). The intersection points of the blue curves with the orange curves represent solutions of (4.36). Stable and metastable solutions are indicated by black and magenta colored dots, respectively. B_0 is the value of B for which the central bulges of the curves would touch (bet. 3rd and 4th plot). Plots are for $N = 7$ and $T = 0.9$, and for $B = 0.2, 0, -0.4, -2, -3$ (note that $B_0 \simeq -1.01$ and $B(x_+) \simeq -2.62$) in units of T_0.

additional row. Further, such states may coexist with a one-row state and be either globally stable or metastable.

All cases refer to plots in Fig. 13. The blue and orange curves represent the solutions of the first and second equation in (4.36), resp. The orange line $y = -ax$, in particular, solves the second equation in the system (4.36) while the first one reduces to the one for the one-row configuration (4.20). Intersections of blue and orange lines represent the solutions the (4.36). Only locally stable solutions are considered.

- $B > 0$: We recover the known one-row solution on the $y = -ax$ line for $x > 0$. There is also a metastable two-row solution with $x < 0$, $y > 0$.
- $B = 0$: The system is symmetric under $x \leftrightarrow y$ and we recover the known one-row solution on the $y = -ax$ line for $x > 0$. There is also a stable solution on the $y = -x/a$ line for $x < 0$, which is equivalent to the previous one, representing spontaneous magnetization in direction x_2.
- $B(x_+) < B < 0$: We recover the known one-row solution on the $y = -ax$ line for $x > 0$, but now it is metastable. There is a stable two-row solution with $x < 0$, $y > 0$.
- $B < B(x_+)$: There are no stable one-row solutions, in accordance with region D of the one-row phase diagram of Fig. 12. There is a unique stable two-row solution.

We note that there are no solutions with $x = y$ since this is not a consistent truncation of the system (4.36), unless $B = 0$ in which case we already know that the corresponding two-row solution is unstable. Thus the symmetry breaking pattern $SU(N) \to SU(N-2) \times SU(2) \times U(1)$ is never realized.

Recalling fig. (12), the picture that emerges, at least for $T < T_0$, is that a two-row solution coexists with the one-row solution in both regions C_1, C_2. The two-row solution is metastable in C_2 ($B > 0$) and becomes absolutely stable in C_1 ($B < 0$). The one-row solution is absolutely stable in C_2, becomes metastable in C_1, and ceases to exist in region D, leaving the two-row state as the only stable solution there. The line $B = 0$ is a metastability frontier between one-row and two-row solutions for $T < T_0$. We expect this picture to extend for a range of temperatures $T > T_0$, with a two-row state coexisting with the one-row one outside of region D, although for high enough temperatures the two-row solution should cease to exist.

5. Conclusions

The thermodynamic properties and phase structure of the $SU(N)$ ferromagnet emerge as surprisingly rich and nontrivial, manifesting qualitatively new features compared to the standard $SU(2)$ ferromagnet. The phase structure of the system, in particular, is especially rich and displays various phase transitions. Specifically, at zero magnetic field the system has three critical temperatures (vs. only one for $SU(2)$), one of them signaling a crossover between two metastable states. Spontaneous breaking of the global $SU(N)$ group in the ferromagnetic phase at zero external magnetic fields happens only in the $SU(N) \to SU(N-1) \times U(1)$ channel. In the presence of a nonabelian magnetic field with M nontrivial components ($M < N$), the explicit symmetry breaking (paramagnetic state) is $SU(N) \to SU(N-M) \times U(1)^M$, while the spontaneous breaking (ferromagnetic state) is $SU(N) \to SU(N-M-1) \times U(1)^{M+1}$. Finally, due to the presence of metastable states, the system exhibits hysteresis phenomena both in the magnetic field and in the temperature.

The model studied in this work, and its various generalizations described below, could be relevant in a variety of physical situations. It could serve as a phenomenological model for physical ferromagnets, in which the interaction between atoms is not purely of the dipole type and additional states participate in the dynamics. In such cases, the $SU(N)$ interactions could appear as perturbations on top of the $SU(2)$ dipole interactions, leading to modified thermodynamics. The model could also be relevant to the physics of the quark-gluon plasma [22], which can be described as a fluid of particles carrying $SU(3)$ degrees of freedom, assuming their $SU(3)$ states interact. Exotic applications, such as matrix models and brane models in string theory, can also be envisaged (see, e.g. [23,24]).

Various possible generalizations of the model, relevant to or motivated by potential applications, and related directions for further investigation suggest themselves. They can be organized along various distinct themes: starting with atoms carrying a higher representation of $SU(N)$, generalizing the form of the two-atom interaction, or including three- and higher-atom interactions.

The choice of fundamental representations for each atom was imposed by the physical requirement of invariance of their interaction under common change of basis for the atom states. Its effect on the thermodynamics is to "bias" the properties towards states with a large fundamental content. This manifests, e.g., in the qualitatively different properties of the system under positive and negative magnetic fields (with respect to the system's spontaneous magnetization). Starting with atoms carrying a higher irrep of $SU(N)$ would modify these properties. In partic-

ular, starting with atoms in the adjoint of $SU(N)$ would eliminate this bias altogether. It might also eliminate phases of spontaneous magnetization, and this is worth investigating.

The interaction of atoms $j_{r,a}j_{s,a}$ was isotropic in the group indices a, an implication of the requirement of invariance under change of basis. Anisotropic generalizations of the form (2.2) can also be considered, involving an "inertia tensor" h_{ab} in the group. Clearly this generalization contains the higher representation generalizations of the previous paragraph as special cases. E.g., $SU(2)$ interactions with the atoms in spin-1 states can be equivalently written as $SU(3)$ fundamental atoms with a tensor h_{ab} equal to δ_{ab} when a, b are in the $SU(2)$ subgroup of $SU(3)$ that admits the fundamental of $SU(3)$ as a spin-1 irrep, and zero otherwise. The more interesting special case in which h_{ab} deviates from δ_{ab} only along the directions of the Cartan generators, in the presence of magnetic fields along these directions, seems to be the most motivated and most tractable, and is worth exploring. The phase properties of the model under generic h_{ab} is also an interesting issue.

Including higher than two-body interactions between the atoms is another avenue for generalizations. Physically, such terms would arise from higher orders in the perturbation expansion of atom interactions, and would thus be of subleading magnitude, but the possibility to include them is present. Insisting on invariance under common change of basis and a mean-field approximation would imply that such interactions appear as higher Casimirs of the global $SU(N)$ and/or as higher powers of Casimirs, the most general interaction being a general function $f(C^{(2)}, \cdots, C^{(N-1)})$ of the full set of Casimirs of the global $SU(N)$. These can be readily examined using the formulation in this paper and may lead to models with richer phase structure. An interesting extension of this study is in the context of topological phases nonabelian models. Such topological phases have been proposed in one dimension [25–28] and it would be interesting to see if they exist in higher dimensions.

Another independent direction of investigation is the large-N limit of the model. This could be conceivably relevant to condensed matter situations involving interacting Bose condensates, or to more exotic situations in string theory and quantum gravity. The presence of two large parameters, n and N, presents the possibility of different scaling limits. These will be explored in an upcoming publication.

Finally, the nontrivial and novel features of this system offer a wide arena for experimental verification and suggest a rich set of possible experiments. The experimental realization of this model, or the demonstration of its relevance to existing systems, remain as the most interesting and physically relevant open issues.

CRediT authorship contribution statement

The two authors contributed equally in the work.

Declaration of competing interest

The authors declare that they have no known competing financial interests or personal relationships that could have appeared to influence the work reported in this paper.

Data availability

No data was used for the research described in the article.

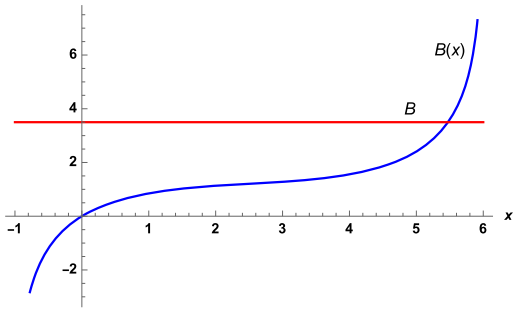

Fig. 14. Plot of $B(x)$ for $T > T_+$.

Acknowledgements

We would like to thank I. Bars for a very useful correspondence, D. Zoakos for help with numerics, and the anonymous Reviewer for comments and suggestions that helped improve the manuscript.

A.P. would like to thank the Physics Department of the U. of Athens for hospitality during the initial stages of this work. His visit was financially supported by a Greek Diaspora Fellowship Program (GDFP) Fellowship.

The research of A.P. was supported in part by the National Science Foundation under grant NSF-PHY-2112729 and by PSC-CUNY grants 65109-00 53 and 6D136-00 02.

The research of K.S. was supported by the Hellenic Foundation for Research and Innovation (H.F.R.I.) under the "First Call for H.F.R.I. Research Projects to support Faculty members and Researchers and the procurement of high-cost research equipment grant" (MIS 1857, Project Number: 16519).

Appendix A. Analysis of one-row states with a magnetic field

In this appendix we present the details of the analysis that we have summarized in the main text.

$T > T_+$ (Fig. 14): $B(x)$ is increasing and all values of x are stable, so there exists a unique stable solution for all B, one-row for $B > 0$ and its conjugate for $B < 0$.

$T_- < T < T_+$ (Fig. 15): We have stability for $-1 < x < x_-$ and $x_+ < x < N-1$, the regions of increasing $B(x)$. Further, note that $x_- > 0$ and $B(x_-) > B(x_+)$, and that $B(x_-) > 0$ while $B(x_+)$ can be positive or negative. The critical temperature T_c satisfies the condition

$$T = T_c \quad \Longleftrightarrow \quad B(x_+) = 0\,, \tag{A.1}$$

which is precisely the condition (3.8). Note that, for $N > 4$, $T_- < T_c < T_+$. For $T > T_c$, $B(x_+) > 0$ and for $T < T_c$, $B(x_+) < 0$.

So within this temperature range we distinguish two sub-cases:

$T_c < T < T_+$ (left plot in Fig. 15): we have for various values of the magnetic field:

- For $B < 0$, x varies from -1 to 0 and there is a unique stable solution corresponding to the conjugate one-row YT.
- For $0 < B < B(x_+)$, x varies from 0 to some $x < x_-$ and there is a unique stable solution corresponding to a one-row YT.

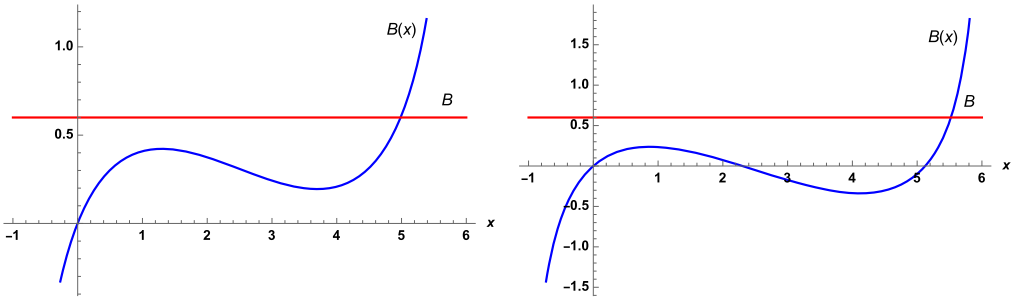

Fig. 15. Plot of $B(x)$ for $T_c < T < T_+$ (Left) and for $T_- < T < T_c$ (Right).

- For $B(x_+) < B < B(x_-)$ we have two locally stable solutions, one for some $0 < x < x_-$ and one for some $x > x_+$ (a third solution in between is unstable). The first one corresponds to an unbroken phase, as it represents a continuous deformation of the singlet for $B = 0$, and the second one to a broken phase. One is absolutely stable and the other metastable. To decide which, we need to compare their free energies.
- For $B > B(x_-)$, x varies from some value greater than x_+ to $N - 1$ and there is a unique stable solution.
  Note that for $B = 0$ there is only the solution $x = 0$, as expected.

$T_- < T < T_c$ (right plot in Fig. 15): we have for various values of the magnetic field:

- For $B < B(x_+)$, x varies from -1 to some negative value x obtained from $B(x_+) = B(x)$ and there is a unique stable solution corresponding to the conjugate one-row YT.
- For $B(x_+) < B < B(x_-)$ we have two locally stable solutions, one for some $x < x_-$ and one for some $x > x_+$. The first one represents an unbroken phase and the second one a broken phase, as they map to the singlet and the one-row solutions for $B = 0$. One is absolutely stable and the other metastable. To decide, we need to compare their free energies.
- For $B > B(x_-)$, x varies from some $x > x_+$ to $N - 1$ and there is a unique stable solution corresponding to a one-row YT.
  Note that $B = 0$ is in the range $B(x_+) < B < B(x_-)$ and we recover the expected two solutions, $x = 0$ (singlet) and $x > 0$ (one-row).

$T_0 < T < T_-$ (Fig. 16): The situation is as in case $T_- < T < T_c$, except now x cannot be more negative than $x_0 = (N - 1)(1 - T/T_0)$ defined in (4.25). The relative size of $B(x_0)$ and $B(x_+)$ will also play a role:

- For $B < \min\{B(x_0), B(x_+)\}$ there is *no* stable one-row solution and the stable solution must necessarily have more rows. According to the general stability analysis, it must be one with $N - 1$ rows out of which $N - 2$ have equal length.
- For $\min\{B(x_0), B(x_+)\} < B < \max\{B(x_0), B(x_+)\}$ there is one stable solution, for $x < 0$ ($x > x_+$) if $B(x_0) < B(x_+)$ ($B(x_0) > B(x_+)$).
- For $\max\{B(x_0), B(x_+)\} < B < B(x_-)$ there are two stable solutions, one absolutely stable and the other metastable. To decide, we need to compare their free energy.
- For $B > B(x_-)$, x there is a single stable solution varying from some $x > x_+$ to $N - 1$.

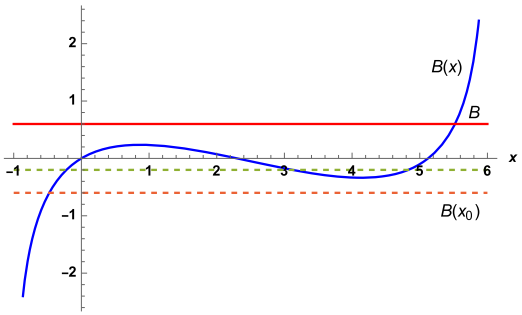

Fig. 16. Plot of $B(x)$ for $T_0 < T < T_-$. The dashed lines refer to the value $B(x_0)$ which could be higher (green) or lower (red) than $B(x_+)$.

$T < T_0$: Only $x > x_+$ solutions are stable.

- For $B < B(x_+)$ there is *no* stable one-row solution, and the solution must again be one with $(N-1)$-rows.
- For $B > B(x_+)$ there is one stable solution for $x > x_+$

A.1. Resolving metastability

To determine which configuration is absolutely stable and which is metastable when there are two locally stable solutions, we need to compare their free energies. The free energy of the system is given by (3.24) with the addition of the magnetic field term,

$$\begin{aligned} F_{\rm sym}(x,T) =& \frac{T}{1+a}\big(a(1+x)\ln(1+x) + (1-ax)\ln(1-ax)\big) \\ & - \frac{a}{2}T_0 x^2 - \frac{B(x)}{N}x - T\ln N \ , \end{aligned} \tag{A.2}$$

where $a = 1/(N-1)$ and where $B = B(x)$ is expressed in terms of x, T via (4.28).

To facilitate the comparison, define the modified free energy Φ (we use $F(x)$ instead of $F_{\rm sym}(x,T)$ for notational convenience)

$$\Phi(x) = F(x) + \frac{N-2}{2N}B(x) \ . \tag{A.3}$$

We can show that $\Phi(x)$ and $B(x)$ satisfy

$$\Phi(N-2-x) = \Phi(x) \tag{A.4}$$

and

$$B(x) + B(N-2-x) = 2T\ln(N-1) - T_0\frac{N(N-2)}{N-1} \ . \tag{A.5}$$

For two solutions with different x, x' but the same B, $F(x) - F(x') = \Phi(x) - \Phi(x')$, so we can compare their Φ to resolve metastability. At the transition point, when the two solutions have the same free energy, (A.4) implies

$$\Phi(x) = \Phi(x') \quad \Longrightarrow \quad x' = N-2-x \tag{A.6}$$

and from (A.5) with $B(x) = B(x') = B(N-2-x)$ the magnetic field B_t at which this happens is

$$B_t = T\,\ln(N-1) - \frac{T_0}{2}\frac{N(N-2)}{N-1}\,. \tag{A.7}$$

For fixed B, this gives the transition temperature T_t at which the two solutions will transit from stable to metastable as

$$T_t = \frac{1}{\ln(N-1)}\left(B + T_0\,\frac{N(N-2)}{2(N-1)}\right)\,. \tag{A.8}$$

For $B = 0$ this reproduces the temperature T_1 and magnetization x_1 that we determined before in (3.27).

Appendix B. Analysis of two-row states in a magnetic field

In this appendix we investigate in detail two-row solutions, including their $(N-1)$-row conjugates. We analyze the conditions for their stability, present the corresponding YT of their irreps, and derive numerical results for the case of temperatures $T < T_0$.

To proceed, we write the coefficients C_i defined in (3.14) in terms of the variables x and y of (4.35). We obtain

$$\begin{aligned} &C_1^{-1} = N\,A(x)\,, \qquad C_2^{-1} = N\,A(y)\,,\\ &C_i^{-1} = N\,A\big(-\alpha(x+y)\big)\,, \qquad i = 3,4,\ldots,N\,, \end{aligned} \tag{B.1}$$

with our usual $A(x)$ defined in (3.19). The variables x and y are restricted by the conditions $0 < x_i < 1$ to the range

$$x, y > -1\,, \qquad x + y < \frac{1}{\alpha} = N-2\,. \tag{B.2}$$

Thus, the allowed solutions are within the triangle in the (x, y)-plane with corners at the points $(1/a, -1)$, $(-1, 1/a)$ and $(-1, -1)$, depicted in Fig. 17. This triangle is further subdivided by the curves $y = x$, $y = -ax$ and $y = -x/a$ into six regions representing the possible ordering of x_1, x_2, x_i $(i \geqslant 3)$ and thus the various YT renditions of the two-row solution. These regions are accordingly labeled by (ijk) for $x_i > x_j > x_k$. Assuming $N > 3$, most of the C_i's are proportional to $1/A(-\alpha(x+y))$, so we choose solutions with $A(-\alpha(x+y)) > 0$. Then at most one of the functions $A(x)$ and $A(y)$ can be negative. We list below the various possibilities together with conditions for stability:

Region A, or (123): $x_1 > x_2 > x_3$, with

$$-ax < y < x \quad\Longrightarrow\quad A(x) < A(y) < A(-\alpha(x+y))\,. \tag{B.3}$$

The stability condition is

$$A(y) > 0\,, \qquad \alpha[A(x) + A(y)]A(-\alpha(x+y)) + A(x)A(y) > 0\,. \tag{B.4}$$

In this region all C_i's are positive, except C_1 which may have either sign. We define

$$\ell_1 = \frac{(1+\alpha)x + \alpha y}{N}\,, \qquad \ell_2 = \frac{(1+\alpha)y + \alpha x}{N}\,, \qquad \ell_1 > \ell_2 > 0\,. \tag{B.5}$$

The YT has the partition

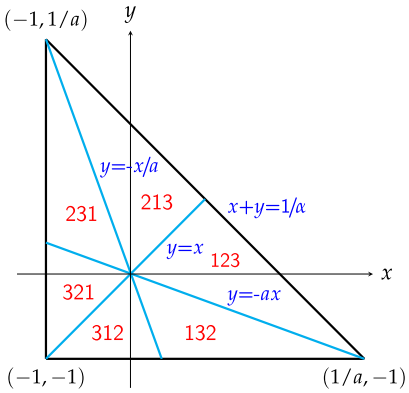

Fig. 17. The domain of x, y. Coordinate axes do not create subdivisions.

$$(\ell_1, \ell_2)\ . \tag{B.6}$$

Hence, it represents a two-row YT with ℓ_1 and ℓ_2 boxes, respectively. This follows from the fact that x_3 is the smallest among the three x_i's and appears $N-2$ times.
Region B, or (132): $x_1 > x_3 > x_2$, with

$$-x/a < y < -ax\ , \qquad A(x) < A(-\alpha(x+y)) < A(y)\ . \tag{B.7}$$

The stability condition is

$$A(-\alpha(x+y) > 0\ , \qquad \alpha[A(x)+A(y)]A(-\alpha(x+y)) + A(x)A(y) > 0\ . \tag{B.8}$$

In this region all C_i's are positive expect C_1 which may have either sign. We define

$$\ell_1 = \frac{x-y}{N}\ , \qquad \ell_2 = -\frac{(1+\alpha)y+\alpha x}{N}\ , \qquad \ell_1 > \ell_2 > 0\ . \tag{B.9}$$

The $(N-1)$-row YT has the partition

$$(\ell_1, \underbrace{\ell_2, \ell_2, \ldots, \ell_2}_{N-2})\ . \tag{B.10}$$

Hence, it represents a YT with ℓ_1 boxes in the first line and ℓ_2 boxes in the following $N-2$ lines. This follows from the fact that the smallest among the three x_i's, x_2 appears only once.
Region C, or (213): $x_2 > x_1 > x_3$, with

$$-ay < x < y\ , \qquad A(y) < A(x) < A(-\alpha(x+y))\ . \tag{B.11}$$

The stability condition is

$$A(x) > 0\ , \qquad \alpha[A(x)+A(y)]A(-\alpha(x+y)) + A(x)A(y) > 0\ . \tag{B.12}$$

In this region all C_i's are positive expect C_2 which could be either positive or negative. Defining

$$\ell_1 = \frac{(1+\alpha)y+\alpha x}{N}\ , \qquad \ell_2 = \frac{(1+\alpha)x+\alpha y}{N}\ , \qquad \ell_1 > \ell_2 > 0\ , \tag{B.13}$$

this case represents a two-row YT with the partition (B.6).

Region D, or (231): $x_2 > x_3 > x_1$, with

$$-ax < y < -x/a \ , \qquad A(y) < A(-\alpha(x+y)) < A(x) \ . \tag{B.14}$$

The stability condition is

$$A(-\alpha(x+y) > 0 \ , \qquad \alpha[A(x)+A(y)]A(-\alpha(x+y)) + A(x)A(y) > 0 \ . \tag{B.15}$$

In this region all C_i's are positive expect C_2 which could be either positive or negative. Defining

$$\ell_1 = \frac{y-x}{N} \ , \qquad \ell_2 = -\frac{(1+\alpha)x+\alpha y}{N} \ , \qquad \ell_1 > \ell_2 > 0 \ , \tag{B.16}$$

this case represents a YT with the partition (B.10).

Region E, or (312): $x_3 > x_1 > x_2$, with $y < x < -ay$, equivalently $x_3 > x_1 > x_2$, with

$$y < x < -ay \ , \qquad A(-\alpha(x+y)) < A(x) < A(y) \ . \tag{B.17}$$

The stability condition is

$$A(-\alpha(x+y)) > 0 \ . \tag{B.18}$$

In these two regions all C_i's are positive. Defining

$$\ell_1 = -\frac{(1+\alpha)y+\alpha x}{N} \ , \qquad \ell_2 = \frac{x-y}{N} \ , \qquad \ell_1 > \ell_2 > 0 \ , \tag{B.19}$$

this case represents a $(N-1)$-row YT with the partition

$$(\underbrace{\ell_1, \ell_1, \ldots, \ell_1}_{N-2}, \ell_2) \ , \tag{B.20}$$

Region F, or (321): $x_3 > x_2 > x_1$, with

$$x < y < -ax \qquad A(-\alpha(x+y)) < A(y) < A(x) \ . \tag{B.21}$$

The stability condition is

$$A(-\alpha(x+y)) > 0 \ . \tag{B.22}$$

In these two regions all C_i's are positive. Defining

$$\ell_1 = -\frac{(1+\alpha)x+\alpha y}{N} \ , \qquad \ell_2 = \frac{y-x}{N} \ , \qquad \ell_1 > \ell_2 > 0 \ , \tag{B.23}$$

this case represents a $(N-1)$-row YT with the partition (B.20).

B.1. The case of low temperatures

We consider temperatures $T < T_0$ for which spontaneous magnetization exists. Various cases arise depending on the sign of B and, if negative, on the value $B(x_+) < 0$ with x_+ defined in (4.24) (recall that $B(x_+)$ is negative for $T < T_0$) and some other intermediate value B_0 to be defined shortly. In the plots below all points on the red line $y = -ax$ solve identically the second equation in the system (4.36), whereas the first one reduces to the equation for the one-row configuration (4.20). This line can be approached for $x > 0$ from the regions A and B and for $x < 0$ from the regions D and F. In addition, the stability conditions for these regions reduce to those in (4.22). All cases below map to one of the plots in Fig. 13.

- $B > 0$: We know that the one-row configuration has a stable solution which in this two-parameter plot is on the $y = -ax$ red line for $x > 0$. The intersection point in the middle (region C in Fig. 17) is unstable, whereas that on the upper left corner is, having a higher value for the free energy, metastable (region C).
- $B = 0$: We have included the case with $B = 0$, which is symmetric with respect to the $y = x$ line. We know that the one-row configuration has a stable solution which in this two-parameter plot is on the $y = -ax$ red line for $x > 0$. Due to the above symmetry there is stable solution also on the $y = -x/a$ line for $x < 0$, which however is equivalent to the above. The other three intersecting points are unstable.
- $B_0 < B < 0$: The value of the magnetic field B_0 arises when the two curves in the plot meet tangentially. The one-row configuration has a stable solution which in this two-parameter plot is on the $y = -ax$ red line for $x > 0$. However, this becomes now metastable, as the stable intersection point is on the upper left corner (region D in Fig. 17), corresponding to an $(N-1)$-row YT with partition (B.10). The other intersection points are unstable.
- $B(x_+) < B < B_0$: There are typically three intersection points along the $y = -ax$ line corresponding to the one-row configuration, the far right is now metastable and the other two unstable. However, there are two additional intersecting points in the far left of that plot, the lower one being unstable and the upper one stable (region D in Fig. 17) corresponding to an $(N-1)$-row YT with partition (B.10).
- $B < B(x_+)$: There is one intersection points along the $y = -ax$ line corresponding to the one-row configuration. This has $x < 0$ and is, as we have shown unstable. In fact, there is no stable one-row configurations for $B < B(x_+)$. Among the other two intersection points the lower one is unstable and the upper one is stable (region D in Fig. 17) and again it corresponds to a $(N-1)$-row YT with partition (B.10).

References

[1] I.I. Lungu, A.M. Grumezescu, C. Fleaca, Unexpected ferromagnetism – a review, Appl. Sci. 11 (15) (2021) 6707.
[2] A.P. Polychronakos, K. Sfetsos, Composing arbitrarily many $SU(N)$ fundamentals, arXiv:2305.19345 [hep-th].
[3] M.A. Cazalilla, A.F. Ho, M. Ueda, Ultracold gases of ytterbium: ferromagnetism and Mott states in an $SU(6)$ Fermi system, New J. Phys. 11 (2009) 103033.
[4] A.V. Gorshkov, et al., Two-orbital SU(N) magnetism with ultracold alkaline-earth atoms, Nat. Phys. 6 (2010) 289–295.
[5] X. Zhang, et al., Spectroscopic observation of $SU(N)$-symmetric interactions in Sr orbital magnetism, Science 345 (6203) (2014) 1467.
[6] M.A. Cazalilla, A.M. Rey, Ultracold Fermi gases with emergent $SU(N)$ symmetry, Rep. Prog. Phys. 77 (2014) 124401.
[7] S. Capponi, P. Lecheminant, K. Totsuka, Phases of one-dimensional SU(N) cold atomic Fermi gases - from molecular Luttinger liquids to topological phases, Ann. Phys. 367 (2016) 50–95.
[8] H. Katsura, A. Tanaka, Nagaoka states in the $SU(n)$ Hubbard model, Phys. Rev. A 87 (2013) 013617.
[9] E. Bobrow, K. Stubis, Y. Li, Exact results on itinerant ferromagnetism and the 15-puzzle problem, Phys. Rev. B 98 (2018) 180101(R).
[10] C. Romen, A.M. Läuchli, Structure of spin correlations in high-temperature $SU(N)$ quantum magnets, Phys. Rev. Res. 2 (2020) 043009.
[11] D. Yamamoto, C. Suzuki, G. Marmorini, S. Okazaki, N. Furukawa, Quantum and thermal phase transitions of the triangular $SU(3)$ Heisenberg model under magnetic fields, Phys. Rev. Lett. 125 (2020) 057204.
[12] K. Tamura, H. Katsura, Ferromagnetism in d-dimensional $SU(n)$ Hubbard models with nearly flat bands, J. Stat. Phys. 182 (2021) 16.
[13] K. Totsuka, Ferromagnetism in the $SU(N)$ Kondo lattice model: $SU(N)$ double exchange and supersymmetry, Phys. Rev. A 107 (2023) 033317.

[14] K. Tamura, H. Katsura, Flat-band ferromagnetism in the SU(N) Hubbard and Kondo lattice models, arXiv:2303.15820 [cond-mat].
[15] D. Yamamoto, et al., Quantum and thermal phase transitions of the triangular $SU(3)$ Heisenberg model under magnetic fields, Phys. Rev. Lett. 125 (2020) 057204.
[16] Y. Miyazaki, et al., Linear flavor-wave analysis of $SU(4)$-symmetric tetramer model with population imbalance, J. Phys. Soc. Jpn. 91 (2022) 073702.
[17] H. Motegi, et al., Thermal Ising transition in two-dimensional $SU(3)$ Fermi lattice gases with population imbalance, arXiv:2209.05919 [cond-mat].
[18] A.P. Polychronakos, K. Sfetsos, Composition of many spins, random walks and statistics, Nucl. Phys. B 913 (2016) 664–693, arXiv:1609.04702 [hep-th].
[19] T. Curtright, T.S. Van Kortryk, C.K. Zachos, Spin multiplicities, Phys. Lett. A 381 (2017) 422–427, arXiv:1607.05849 [hep-th].
[20] V. Holten, C.E. Bertrand, M.A. Anisimov, J.V. Sengers, Thermodynamics of supercooled water, J. Chem. Phys. 136 (2012) 094507, arXiv:1111.5587 [physics].
[21] See, e.g., Feynman lectures (ch. 36).
[22] R. Pasechnik, Michal Šumbera, Phenomenological review on quark-gluon plasma: concepts vs. observations, Universe 3 (2017) 7, arXiv:1611.01533 [hep-ph].
[23] See, e.g., E. Martinec, Matrix models and 2D string theory, in: Application of random matrices in physics, NATO Advanced Study Institute, Les Houches, France, June 6–25, 2004, pp. 403–457, arXiv:hep-th/0410136.
[24] G.J. Turiaci, M. Usatyuk, W.W. Weng, Dilaton-gravity, deformations of the minimal string, and matrix models, Class. Quantum Gravity 38 (20) (2021), arXiv:2011.06038 [hep-ph].
[25] A. Roy, T. Quella, Chiral Haldane phases of $SU(N)$ quantum spin chains, Phys. Rev. B 97 (2018) 155148.
[26] S. Capponi, P. Fromholz, P. Lecheminant, K. Totsuka, Symmetry-protected topological phases in a two-leg SU(N) spin ladder with unequal spins, Phys. Rev. B 101 (2020) 195121.
[27] K. Totsuka, P. Lecheminant, S. Capponi, Semiclassical approach to competing orders in a two-leg spin ladder with ring exchange, Phys. Rev. B 86 (2012) 014435.
[28] K. Remund, R. Pohle, Y. Akagi, J. Romhanyi, N. Shannon, Semi-classical simulation of spin-1 magnets, Phys. Rev. Res. 4 (2022) 033106.